RELATÓRIO DE PESQUISA

Estudo das Propriedades Ópticas em Alexandrita ($BeAl_2O_4:Cr^{3+}$) comparado com Crisoberilos ($BeAl_2O_4$)

Relatório de Pesquisa do Prof. Dr. Neilo Marcos Trindade (IFSP) apresentado para pós doutoramento sob a orientação da Profa. Dra. Elisabeth M. Youshimura junto ao Departamento de Física Nuclear do Instituto de Física da Universidade de São Paulo.

Fevereiro/2017

Sumário

RESUMO

Alexandrita é um mineral da variedade crisoberilo que contém cromo em sua estrutura, possuindo a seguinte composição química: $BeAl_2O_4:Cr^{3+}$. O Brasil é considerado atualmente o maior produtor mundial de alexandrita; porém, ainda é uma gema pouco conhecida quanto as suas propriedades físicas. Além de apresentar um efeito de mudança de cor dependendo da fonte de luz a qual esta exposta, esse material também tem sido importante tecnologicamente como laser em aplicações médicas, principalmente na área de dermatologia e tratamento de câncer, com propriedades superiores aos seus principais concorrentes, lasers de rubi e Nd:YAG. Nesse trabalho a composição química das amostras serão obtidas pela técnica de fluorescência de raios X e a qualidade das amostras será verificada por meio de absorção óptica na região do visível. O objetivo da pesquisa é investigar os efeitos de radiação ionizante (raios X, beta e gama) e da luz UV em propriedades ópticas de alexandrita utilizando técnicas de Termoluminescência (TL) e Luminescência Opticamente Estimulada (OSL). O projeto tem também como objetivo correlacionar e ampliar os conhecimentos sobre esse material, principalmente quanto a resposta luminescente - TL e OSL - e o estudo da viabilidade de uso em dosimetria de radiações. Estudos preliminares mostram que alexandrita exibe picos TL de baixa intensidade em 110, 160 e 280˚C e um pico dominante em 350˚C e resultados inéditos de OSL mostram um sinal intenso no espectro mesmo com doses baixas de radiação. Acredita-se que as impurezas, principalmente o Cr^{3+} e Fe^{3+}, têm um papel importante nessas características.

1. REALIZAÇÕES NO PERIODO

O Brasil é considerado atualmente o maior produtor mundial de alexandrita ($BeAl_2O_4:Cr^{3+}$). O objetivo da pesquisa é investigar os efeitos de radiação ionizante (raios X, beta e gama) e da luz UV em propriedades ópticas de alexandrita utilizando técnicas de TL e OSL, e o estudo da viabilidade de uso em dosimetria de radiações. A investigação da potencialidade da alexandrita como material dosimétrico é relevante por alguns aspectos; mapear o material quanto a determinação dos picos TL e a curva resposta com a dose; há uma escassa literatura sobre a técnica TL aplicada a esse material, e não consta publicações de OSL para o mesmo material; e o fato de que a matriz contém 19,8 wt% de BeO e 80.2 wt% de Al_2O_3, ambos muito utilizado na área de dosimetria TL e OSL.

O grupo possui uma grande quantidade de amostras naturais oriundas do estado da Bahia e de Minas Gerais, Brasil. Para efeito de comparação, será utilizado uma amostra sintética, crescida por H. P. Jenssen and R. Morris (Allied Signal Inc, U.S.A.), pelo método Czochralski. As análises químicas são realizadas através de medidas de fluorescência de raios X (XRF), utilizando um espectrômetro MINI-X (modelo Amptek XR-100SDD). As medidas de absorção óptica são realizadas na faixa de 400 a 700 nm, utilizando um espectrofotômetro Cary 1G de Varian. As medições de OSL e TL são realizadas utilizando um leitor comercial de TL/OSL automatizado produzido pelo Laboratório Nacional Risø (modelo DA-20).

Na primeira fase desse pós-doutoramento o candidato publicou o seguinte artigo com o grupo:

Trindade, N.M., Blak, A.R., Yoshimura, E.M., de Andrade Scalvi, L.V. and Scalvi, R.M.F. (2016) Photo-Induced Thermally Stimulated Depolarization Current (TSDC) in Natural and Synthetic Alexandrite ($BeAl_2O_4$:Cr^{3+}). *Materials Sciences and Applications*, 7, 881-894. http://dx.doi.org/10.4236/msa.2016.712067.

Também iniciou os estudos de TL e OSL em alexandrita. Estudos preliminares mostram que o mineral exibe picos TL de baixa intensidade em 110, 160 e 280˚C e um pico dominante em 350˚C e resultados inéditos de OSL mostram um sinal intenso no espectro mesmo com doses baixas de radiação. No momento o candidato está produzindo um artigo referente a esses resultados que será submetido em breve:

Trindade, N.M., Yoshimura, E.M. (2017) TL and OSL preliminar studies on $BeAl_2O_4$:Cr^{3+} natural Brazilian mineral. *Minerals Engineering.*

Esses resultados foram divulgados em eventos científicos nacionais, como Encontro de Física 2016, Brazilian Materials Research Society Meeting, Congresso Brasileiro de Engenharia e Ciência dos Materiais, Brazilian Meeting on Inorganic Chemistry; e serão divulgados em eventos internacionais como Process Mineralogy 17, financiado pela FAPESP processo 2016/22984-0, a ser realizado em março na África do Sul.

2. ANEXOS

- Trindade, N.M., Yoshimura, E.M. (2017) TL and OSL preliminar studies on $BeAl_2O_4$:Cr^{3+} natural Brazilian mineral. *Minerals Engineering* (artigo a ser submetido em março);
- Trindade, N.M., Blak, A.R., Yoshimura, E.M., de Andrade Scalvi, L.V. and Scalvi, R.M.F. (2016) Photo-Induced Thermally Stimulated Depolarization Current (TSDC) in Natural and Synthetic Alexandrite

($BeAl_2O_4:Cr^{3+}$). *Materials Sciences and Applications*, 7, 881-894. http://dx.doi.org/10.4236/msa.2016.712067;

- Certificado de participação no Encontro Nacional de Física 2016;
- Certificado de participação no Brazilian Materials Research Society Meeting;
- Certificado de participação no Congresso Brasileiro de Engenharia e Ciência dos Materiais;
- Certificado de participação no Brazilian Meeting on Inorganic Chemistry;

3. PLANO DE ATIVIDADES

A continuidade deste projeto está prevista para 1 ano. A seguir, encontra-se o quadro de distribuição bimestral das atividades que serão desenvolvidas no decorrer do projeto. Nele, as linhas verticais indicam os semestres e as horizontais significam:

A – Revisão Bibliográfica;

B – Medidas de Termoluminescência (TL);

C – Medidas de Luminescência Opticamente Estimulada (OSL);

D – Paralelamente às medidas de TL e OSL, realização de medidas de Absorção Ótica na região espectral do ultravioleta e visível;

E – Microanálises das amostras naturais através de FRX;

F – Interpretação e submissão dos resultados para revistas cientificas da área.

	1°/ 2017	2°/ 2017
A	■	■
B	■	■
C	■	■
D	■	■
E		■
F		■

4. CONSIDERAÇÕES FINAIS

Espera-se ter demonstrado o mérito do relatório e que a continuidade da pesquisa é muito salutar para que o mesmo possa evoluir na linha de pesquisa escolhida e estabelecer novas parcerias, além de divulgar seu trabalho na comunidade internacional e também ter a oportunidade de publicar.

TL and OSL preliminary studies on $BeAl_2O_4$: Cr^{3+} natural Brazilian mineral

Neilo Marcos Trindade*[a,b] and Elisabeth Mateus Yoshimura[b].

[a] São Paulo Federal Institute - IFSP, Rua Pedro Vicente, 625, 01109010, São Paulo, SP, Brazil
e-mail: ntrindade@ifsp.edu.br
[b] University of São Paulo - USP, Institute of Physics, Rua do Matão, 1371, 05508090, São Paulo, SP, Brazil
e-mail: e.yoshimura@if.usp.br
* corresponding author: +5515997776800. Rua Paulo Varchavtchik 581, 18087190, CS C7, Sorocaba, SP, Brazil.

ABSTRACT

The investigation of luminescent properties in alexandrite ($BeAl_2O_4$:Cr^{3+}) in natural form is presented in this paper. Alexandrite is a rare and precious mineral that changes color according to the light incident on it. Moreover, in the synthetic form it is used technologically as active medium for laser, especially to its applications in the medical field, with properties superior to its main competitors, ruby and Nd:YAG. Sample composition is obtained through X-ray fluorescence measurements and, we present results of optical absorption. The work proposes to examine the behavior of thermoluminescence (TL) and Optically stimulated luminescence (OSL) signals, as well as their correlations. Initial measurements show that alexandrite sample exhibits low intensity TL peaks at 110, 160 and 280˚C and a dominant peak at 350˚C. For the first time an OSL study of the material is performed, showing an intense signal. In addition, probably Fe and Cr ions have an important part in the process TL and OSL.

Keywords: Alexandrite, Crysoberyl, TL, OSL, XRF, Optical absorption.

1. INTRODUTION

Thermoluminescence (TL) is the light emitted by some crystals that were exposed to ionizing radiation, when heated. It is a thermally stimulated emission originating from an energy that was previously stored in the crystal during the irradiation (Yukihara, 2001). Therefore, the exposure of material to ionizing radiation leads to the population of the available trap levels, while heating leads to the release of traps (Jacobsohn *et al.*, 2013). This light emission after heating is caused by the release of charges trapped in defects in insulating or semiconducting materials (Mckeever, 1985) and their recombination with opposite charges in other defects called recombination centers.

Optically stimulated luminescence (OSL) allows complementing the TL characterization through optical stimuli of the irradiated material. The interesting thing about this technique is that the luminescence can be monitored at room temperature, without heating the material, a fact that is used for applications in dating and dosimetry (Yukihara, 2001). OSL is observed during illumination of crystalline insulating materials or crystalline semiconductors that have been previously excited, typically by ionizing radiation (Yukihara & Mckeever, 2011). When the OSL signal is proportional to the absorbed dose, the material in question can be used as a dosimeter. OSL has been observed since the 19th century, but has only been used for dating and personal dosimetry since the mid-20th century (Mckeever, 2001; Mckeever, 2011). Although it is a well-founded knowledge, a wider use of OSL for dosimetry is hampered due to the limited number of dosimetric materials available. The objective of this work is to study the feasibility of a new material, alexandrite mineral, for OSL dosimetry.

Alexandrite, chemical composition: $BeAl_2O_4$: Cr^{3+}, is well known in the medical field in synthetic form as an active laser medium, first reported by Bukin *et al.* (1978), with superior characteristics when compared to other types of media with emission in the range between 700 and 800 nm (Torezan & Osório, 1990; Scalvi *et al.*, 2005). Comprehensive works about applications of the alexandrite laser in medicine can found in papers by Toosi *et al.* (2010), Ibrahimi *et al.* (2011), Nilforoushzadeh (2011), Li *et al.* (2012), Saedi *et al.* (2012), Wang *et al.* (2012) and Kim *et al.* (2014). Another interesting fact about this mineral is its color change according to light incident on it. This property, well known in the literature as alexandrite effect (Gubelin *et al.*, 1976), results in popularity and high market value of alexandrite as a gem (Collins *et al.*, 1997),. However, despite belonging to families of gems of high economic and

technological interest (Ollier *et al.*, 2015), being Brazil one of the largest producers of this mineral there are few studies of the physical properties of natural alexandrite.

The alexandrite structure is of chrysoberyl type with the incorporation of chrome in its lattice (Rossi *et al.*, 2014). Chrysoberyl ($BeAl_2O_4$) has orthorhombic symmetry (*Pmnb*) that corresponds to dense hexagonal packing, influencing the oxygen atom positions, which are slightly distorted by the presence of aluminum atoms. These distortions give rise to two sites of different symmetries: a site, Al_1, set in an inversion center (Ci symmetry) and a site, Al_2, located in a reflection plane (Cs symmetry) (Rabadanov & Dudka, 1997; Ivanov *et al.*, 2005; Scalvi *et al.*, 2007). The larger site, Al_2, is preferably occupied in alexandrite by Cr^{3+} ions which are responsible for the optical properties of alexandrite as laser emission (Shepler, 1984; Scalvi *et al.*, 2002, Weber *et al.*, 2007).

In the literature, although there are many papers related to optical properties in alexandrite, as mentioned before, we found, in our bibliographic search, only one study the ionizing radiation effects in synthetic alexandrite (by Yarovoi *et al.*, 1991), and another paper about thermoluminescence studies on natural alexandrite and crysoberyl (by Ferraz *et al.*, 2002). Further motivation for this work is the fact that crysoberyl contains 19.8 wt % BeO and 80.2 wt % Al_2O_3 (Ivanov *et al.*, 2005). BeO as a good material for TL and OSL dosimetry,with high sensivity to ioniziation radiation, linear dose response and an effective atomic number (Zeff = 7,2) near that of human soft tissue (Zeff ~7,6) (Groppo & Caldas, 2014). By the other hand, Al_2O_3 is a sensitive TLD and OSL material, well established in luminescence dosimetry (Yukihara & Mckeever, 2011), but studies are still being done to improve TL/OSL properties in these materials using different dopants (Salah *et al*., 2011; Liu *et al*., 2013). For example, the Al_2O_3:C is a unique synthetic material in use today as an OSL dosimeter and has applications as in medical, personnel and environmental dosimetry (Yoshimura & Yukihara, 2006); single crystals of Al_2O_3: Fe, Mg, Cr have also shown interesting results (Yoshimura, 2007), and Cr doped Al_2O_3 system has been studied and proposed as a UV and an ionizing radiation dosimeter (Pokorny & Ibarra, 1993). These detectors are used in applications like solar irradiation monitoring, chemical analysis or medical sensing as in phototherapy (Escobar-Alarcón et al., 2003). Salah *et al*. (2011) also propose nanoparticles of Al_2O_3: Cr with easy method of preparation, good sensitivity, simple glow curve structure and useful TL response over a wide range of doses, being a candidate for high dose dosimetry for food and seed irradiation. Moreover, Liu *et al*. (2013) managed to produce Cr:α-Al_2O_3 transparent ceramics and showed that with

increasing Cr_2O_3 content the intensities of TL peaks increased and could improve the stability and sensitivity of its OSL signal.

In this paper, we will present a series of experimental results of TL and OSL of Brazilian alexandrite, relating the observations with the material impurities, to explain the mechanism of the luminescence and the effects of ionizing radiation in this crystal.

2. MATERIALS AND METHODS

Our sample is a stone of alexandrite originated from Bahia state, Brazil, with a dark green color. Two 1.0 mm thickness slides with perfectly parallel faces were cut from this stone, mass around 0.050 g, and denominated as *Ale G* and *Ale H*. Before the first use and between subsequent uses of the same sample in an experiment, the sample was heated at 20ºC/min up to 700ºC and kept at this temperature for 1h, in a muffle furnace, to empty the traps and erase the TL and OSL signals.

Chemical analyses were performed through X-ray fluorescence (XRF) measurements, using a MINI-X spectrometer (Amptek XR-100SDD model). The fluorescence intensities of the characteristic X-rays (Kα lines) were measured with a Si Drift detector (25 mm^2 x 500 μm/0.5 mil) with Be window (1.5”). Optical absorption measurements were carried out in the range 400 to 700nm, using a spectrophotometer Cary 1G of Varian.

OSL and TL measurements were carried out using a commercial automated TL/OSL reader produced by Risø National Laboratory (model DA-20). Luminescence was stimulated using blue light emitting diodes (470 nm, FWHM = 20 nm) delivering 80 mW/cm^2 at the sample position in CW mode. Each OSL measurement was carried out during 60 s of LED stimulation with 90% of the maximum power of. The TL/OSL signals were detected with a bialkali photomultiplier tube (PMT) behind an UV transmitting broad-band glass filter (Hoya U-340, 7.5 mm thick and 45 mm diameter) to block the stimulation light while transmitting part of the OSL signal from the samples. Irradiations were performed at room temperature using the built-in $^{90}Sr/^{90}Y$ beta source of the TL/ OSL reader (dose rate of 10 mGy/s) at a dose range from 10 Gy to 50 Gy. TL glow curves were obtained using a heating rate of 5ºC/s.

3. RESULTS AND DISCUSSION

Figure 1 shows the results of XRF technique used to obtain mainly the concentration of iron, aluminum and chromium contained on the two samples. The technique does not detect Be element due to its low atomic number.

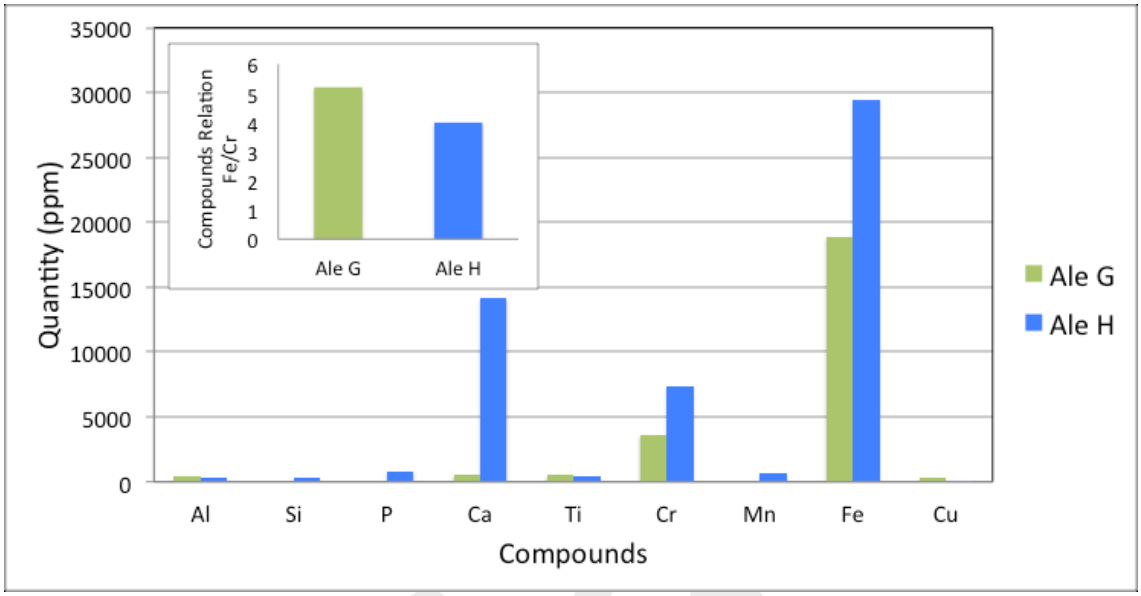

Figure 1: X-ray fluorescence analysis results of *Ale G* and *Ale H* samples of natural alexandrite. The inset shows compounds relation of Fe/Cr for samples.

It is possible to observe by the compositional analysis, that differenty Fe and Cr concentration are present in the two samples. Results like this are expected since natural materials, as the environment, the temperature and other important parameters of the mineral forming process may influence the incorporation in different parts of the stone. Is verified here Si, P, Ca, Ti, Mn, Cu, and a high concentration of Ca is found in sample *Ale H*. Moreover, as seen in the inset of Figure 1, the presence of Fe in these natural samples is substantially large compared to Cr. The Fe presence is very relevant in alexandrite samples, because a high amount of this impurity may mask the identification of optical absorption bands attributed to Cr^{3+} in the host matrix (Trindade *et al*., 2010), and may influence the results of electrical properties of this mineral (Trindade *et al*., 2016). Iron may also play an important role in TL results.

The optical absorption spectrum for natural alexandrite is shown in Figure 2, measured at room temperature.

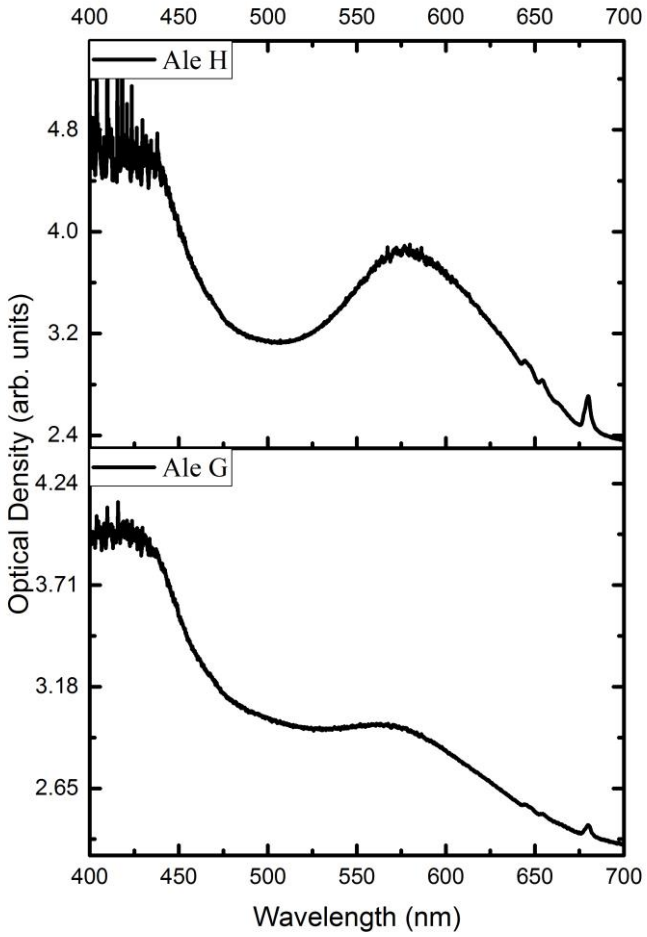

Figure 2: Optical absorption spectra of *Ale G* and *Ale H* samples of natural alexandrite.

In the case of alexandrite, the spectrum is expected to present two wide absorption bands (A and B), and two lines (the R lines). Band A, centered at 590nm represents the overlapping of two absorption bands of Cr^{3+} ions in two distinct sites Al_1 and Al_2, associated with the transition from ground state $^4A_{2g}$ to excited states $^4T_{2g}$. Band B, centered at 420nm represents Cr^{3+} and Fe^{3+} also incorporated at different sites, with the transition from ground state $^4A_{2g}$ to excited states $^4T_{1g}$. The R lines correspond to $^4A_{2g}$ ⇔ ^2E_g transition (Ollier *et al.*, 2015), and show up around 680nm are attributed to Cr^{3+} located at Al_2 sites on a reflection plane, and responsible by optical properties of alexandrite. As experimentally verified and presented in the literature (Powell *et al.*, 1985; Suchocki, 1987), R_1 and R_2 lines (not defined in Figure 2 due to limitation of the experimental apparatus) appear precisely at the same wavelengths (680.4 nm and 678.5, respectively), in both absorption and emission spectra, at room temperature. They are

associated with transitions from the ground state to the ^2E level. The narrow lines that appear at 655.7, 649.3 and 645.2 nm positions in the optical absorption and are associated with Cr^{3+} ions lines in Al_1. The result is in accordance with previously published measurements for both natural and synthetic sample (Trindade *et al.*, 2010), therefore, this outcome is consistent with the known presence of Cr^{3+} in this sample.

The dose-response curves were obtained for TL and OSL techniques and are shown in Figures 3 and 4. The samples were pre-annealed at 700˚C for one hour and then beta irradiated to doses from 10 to 50 Gy.

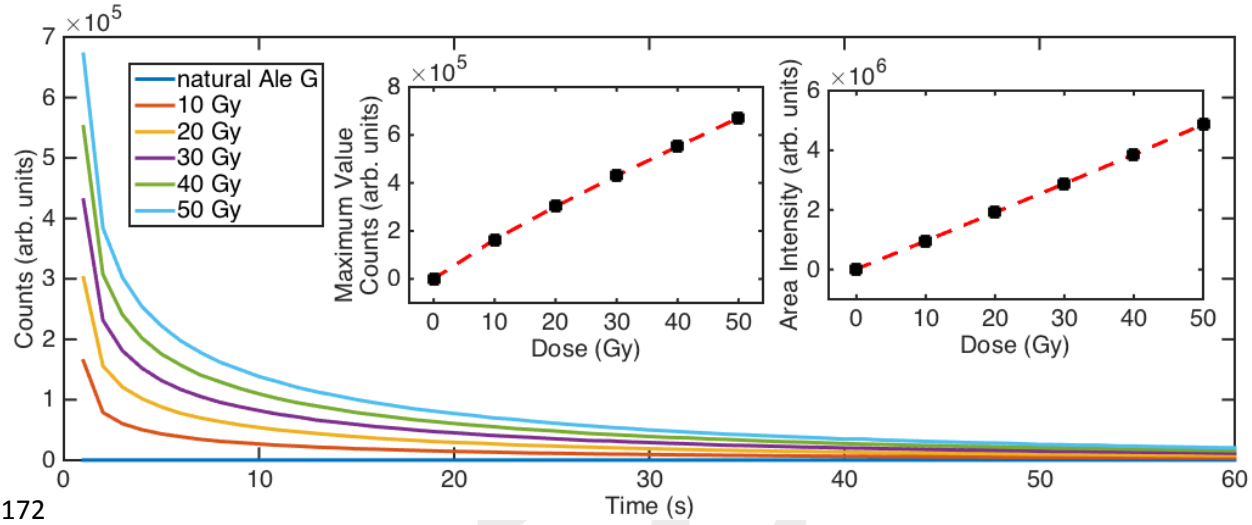

(a)

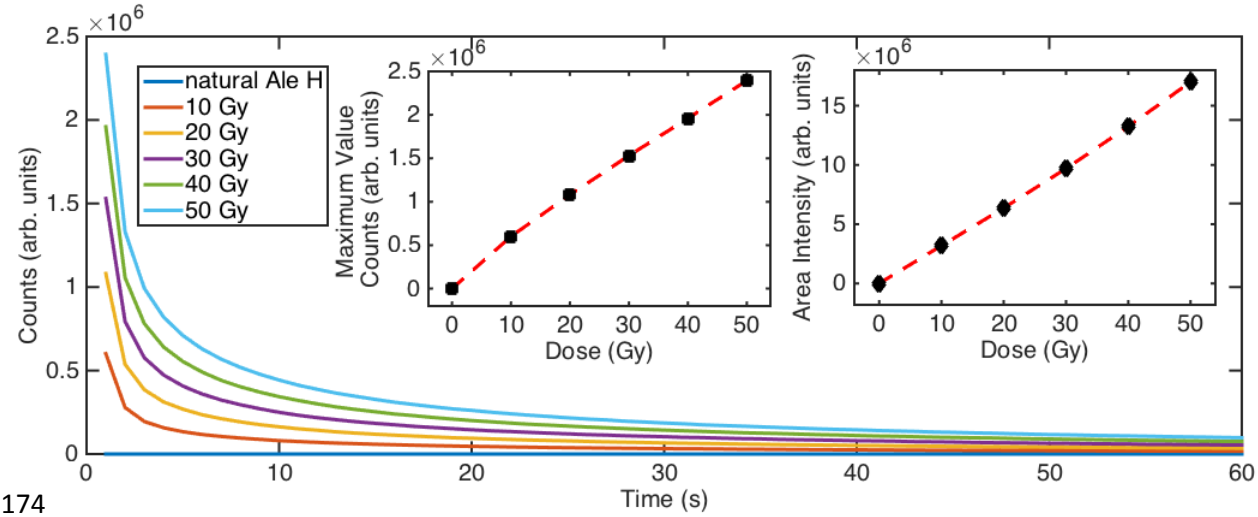

(b)

Figure 3: OSL curves of samples *Ale G* (a) and *Ale H* (b) of natural alexandrite after pre-irradiation treatments with dose, using blue light. The inset shows maximum value counts and area intensity for each curve as a function of dose.

In the OSL curves we can observe that the sample *Ale H* emits more light for the same absorbed dose than the sample *Ale G*. Correlating with the results of XRF this can be related to the amount of Cr and Fe trapping centers that are more quantitative for sample *H* than the *G*. The decay of the counts in the OSL measurement for both samples is similar, starting the curve with intense value and decreasing exponentially to values close to zero after 1 min of the blue light. We also observed that there is linearity in the data when we analyze the plot of area intensity versus dose.

Figure 4 shows the residual TL glow curves obtained.

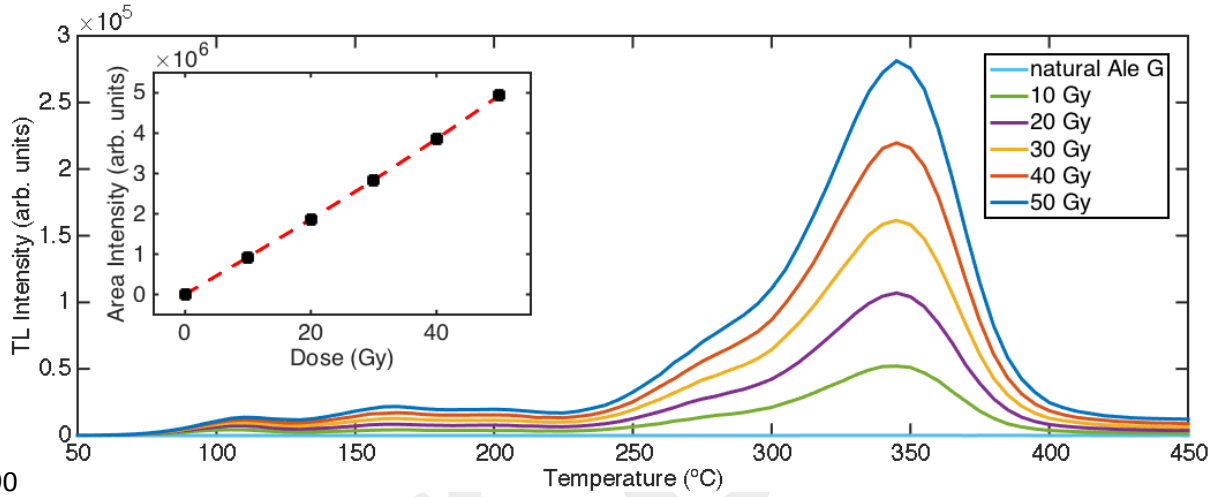

(a)

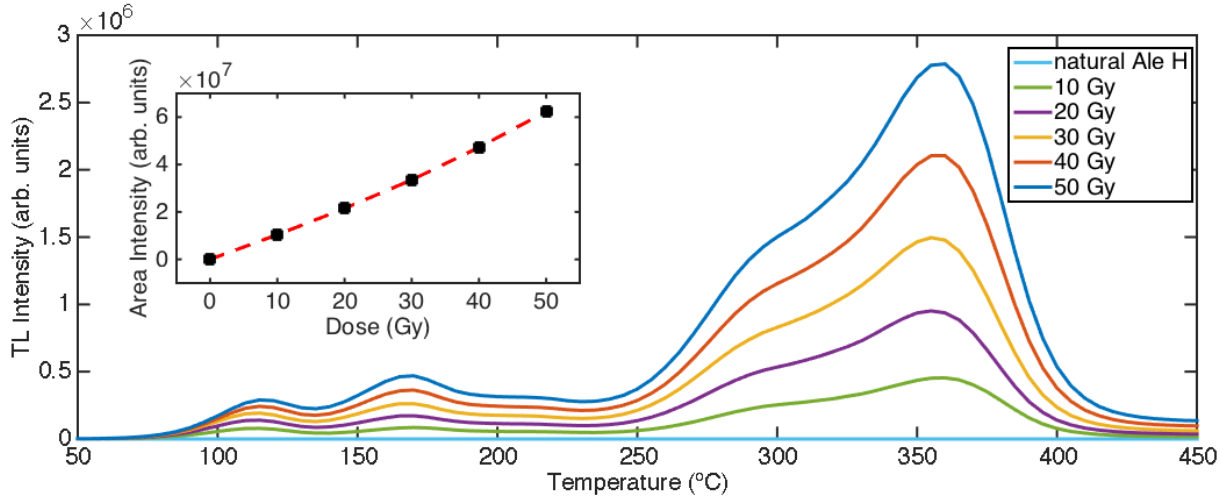

(b)

Figure 4: TL curves of samples *Ale G* and *Ale H* of natural alexandrite after several pre-irradiation treatments with dose, using a 5˚C/s heating rate. The inset shows area intensity for each curve as a function of dose.

Both alexandrite samples show light emission over a very wide temperature range with small peaks at 110, 160 and 280˚C and a dominant peak at 350˚C, the width suggests that the glow curve represents the superposition of several peaks. In inset figure, it is observed that material exhibits a linear growth of TL area intensity with dose

Yoshimura (2007) investigated the emission in aluminum oxide single crystal doped with Cr, Mg and Fe and results show a TL glow curve with at four peaks (110, 160, 225 and 270˚C) and that the trapping center responsible for the 160˚C peak is related to intrinsic defects, and that the other TL glow peak positions are impurity dependent. Villarreal-Barajas *et al*. (2002) show the presence of the temperature peak at 162˚C, glow curve obtained for the beta irradiation in aluminum oxide thin films, with good stability and suggest that this peak can be used as a dosimetric peak. Mittani *et al*. (2002) also observed peak at 165˚C in all the glow curves with different doses for natural beryl exposed gamma irradiation, and this process involves Fe^{3+} ions.

Ferraz *et al*. (2002) suggest that the pre-annealing at temperatures higher than 600˚C induces the $Fe^{2+} \rightarrow Fe^{3+}$ conversion in natural sample and that an increase in the Fe^{3+} ions improves TL emission at 320˚C, this is because these ions are able to capture electrons during irradiation. Pokorny & Ibarra (1994) in their paper report that the presence of the peak at 330˚C in *G* and *H* samples is related to the emission of holes or electrons related to the presence of Cr^{4+} ions, but reference other works in which this peak can appear for Al_2O_3 doped with other impurities or even appears for Al_2O_3 doped with Cr. Finally, they conclude that the peak is related to the F centers and their recombination with Cr^{4+} ions. It is still possible to perceive a band around 275 to 295˚C, Lapraz *et al*. (1991) in their study comment that this peak is attributed by them to a conversion of the Cr^{2+} (or Cr^{4+}) centers for Cr^{3+}.

Figure 5 shows the OSL glow curves of alexandrite pre-annealed at 700˚C for one hour and then beta irradiated to a dose of 1 Gy and kept in the dark before readout for various times (from 5 to 60 min). This study is intended to verify the stability of the OSL signal of both samples and detect if they present fading of the OSL signal.

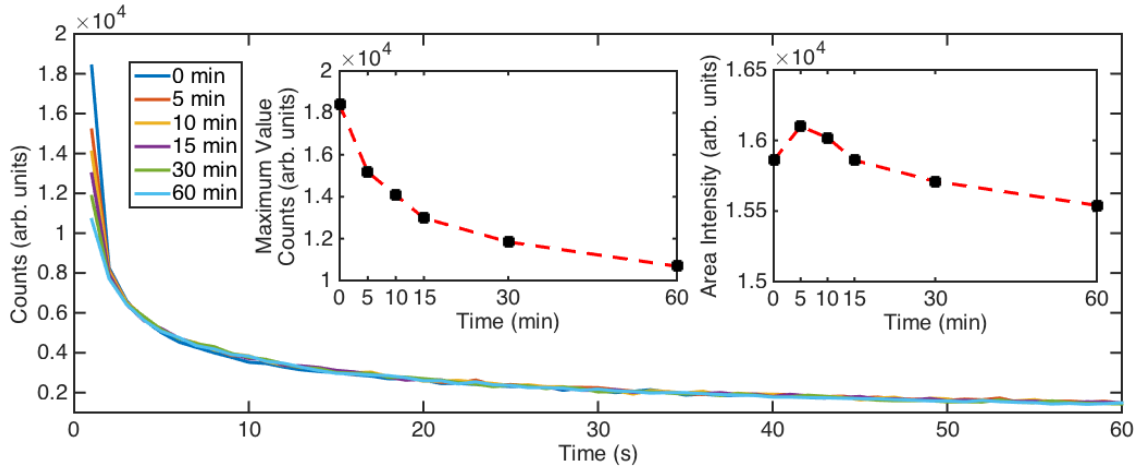

(a)

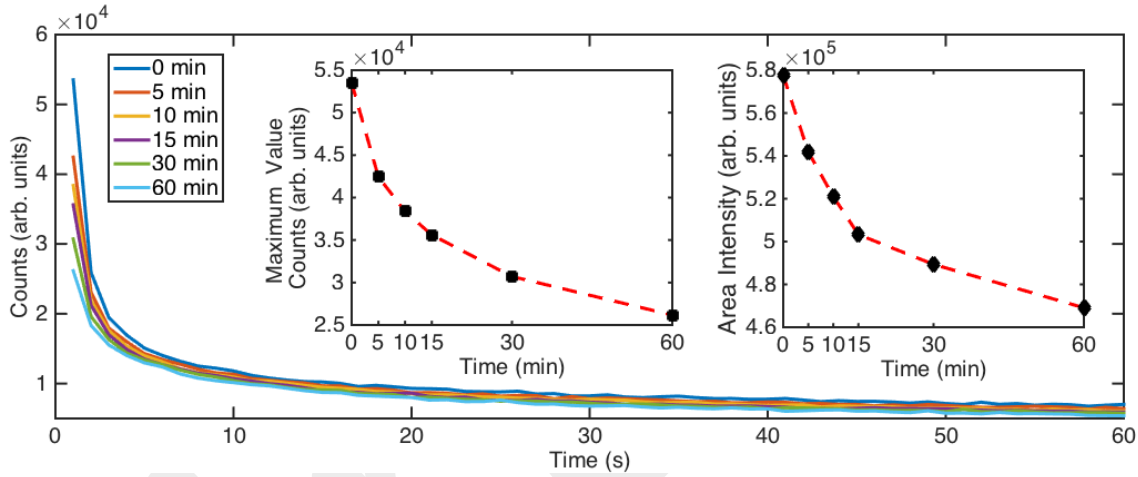

(b)

Figure 5: OSL curves of samples *Ale G* and *Ale H* of natural alexandrite after pre-irradiation treatments with pause, using blue light and dose of 1Gy. The inset shows maximum value counts and area intensity for each curve as a function of pause time.

First, we observed that even with a lower dose, 1Gy, and without any pause between the dose and the OSL measurement, both samples show OSL signal, initiating sample *Ale H* with a higher counts value than sample *Ale G*, in relation the presence of Cr and Fe elements. Although there is a significant decrease of the initial OSL signal for both samples (about 40% decrease for both samples) we notice that, for sample G the decrease of the integral signal is very subtle – less than 5%. The integral signal for sample H has more fading, but it corresponds to less than 20% of loss in 60 min of storage in dark. Although a longer time study can be performed, the residual signal is large enough for dosimetry applications. It is a question of waiting some time for single stabilization or introducing a pretreatment that eliminates the non-stable part of the signal before analysis. In this result, we show that even with a time delay of some

minutes before the OSL reading of the sample it is possible to generate a stable and reproducible OSL signal, but with an intensity reduced in the maximum value of counts and area intensity. It is important to note that *Ale G* sample, when dealing with the reduction in area intensity with time delay, remained more stable than *Ale H* sample. In addition, sample *G* showed complete emptying (close to zero) with the time delay, while sample *H* presented a higher background value, possibly requiring more time for total emptying to occur.

Figure 6 shows the TL glow curves obtained after of the fading study.

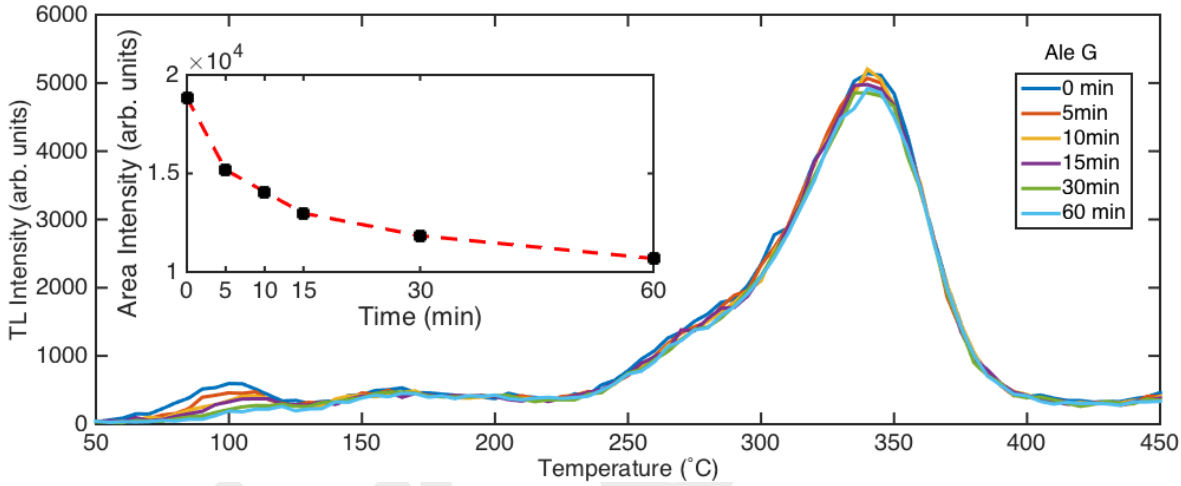

(a)

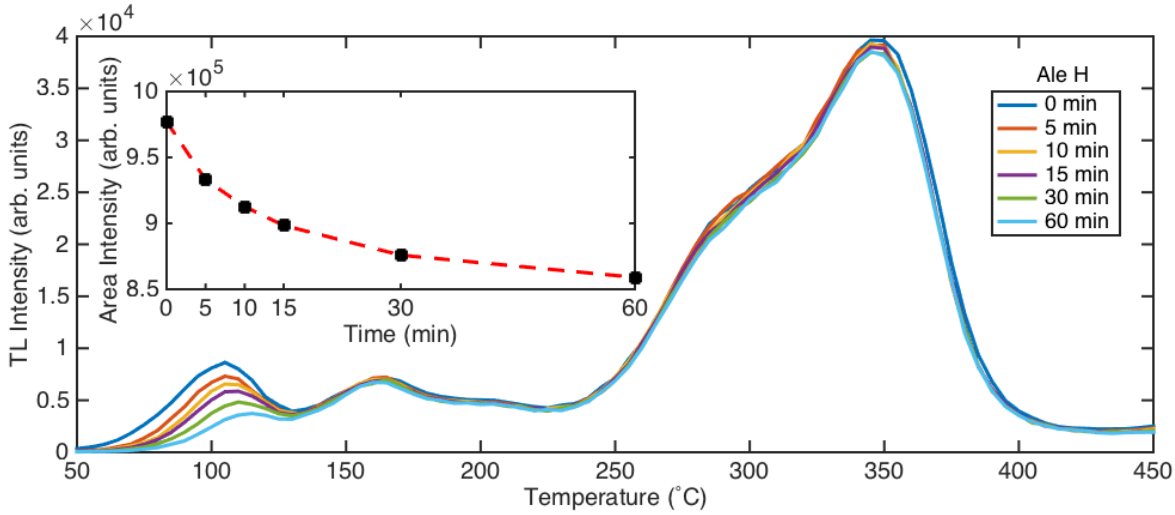

(b)

Figure 6: TL curves of samples *Ale G* and *Ale H* natural alexandrite after several pre-irradiation treatments with pause, using 5˚C/s heating rate and dose 1Gy. The inset shows area intensity for each curve as a function of pause time.

To assist in the interpretation of the previous results, especially the peak at 110˚C, Figure 7 presents the TL analysis with and without blue light (OSL) for one of the samples.

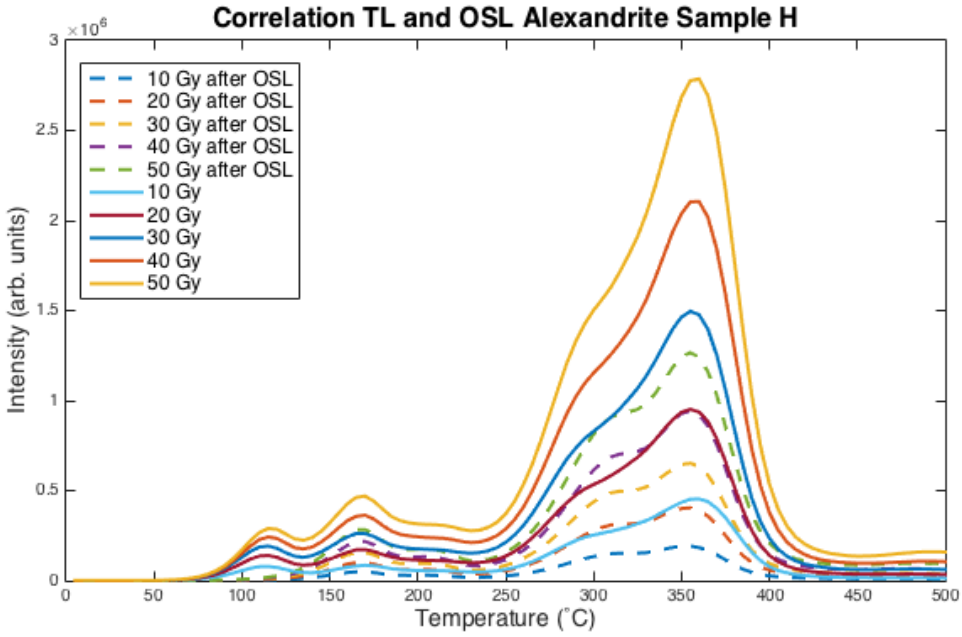

Figure 7: TL curves of samples *Ale H* of natural alexandrite after several pre-irradiation treatments with dose, using a 5˚C/s heating rate, with and without exposure to blue light (OSL).

The first peak at 110˚C is unstable at room temperature. It is possible to observe the differences between the measurements with and without exposure to blue light of OSL. Comparing samples, this peak is more evident in *Ale H* than *Ale G* and we observed that by XRF analysis *Ale H* presents an expressive amount of calcium, therefore, we try to correlate with Rocha *et al*. (2003) that investigated calcium aluminate glass samples to describe the intrinsic defects that are formed in UV irradiated glasses. In our measurement, it is observed that 1 h after irradiation at room temperature there is a drastic reduction of intensity only of that peak, which is evident in the inserted graph of the area intensity with the pause time. If we separate this peak, we observe qualitatively that the area remains constant because the other peaks do not have significant changes in the intensity of the curves. Rocha *et al*. (2003) observed TL glow curves present a broad band centered at 120 ˚C, and just like our case, when the time interval between the sample irradiation and the TL measurement increase, the peak moves towards higher temperatures, emptying of the TL band and indicating the presence of a continues distribution of activation energies.

4. CONCLUSIONS

The X-ray fluorescence analysis revealed elements as Al, Si, P, Ca, Ti, Mn and Cu, particularly Fe and Cr, expected by the chemical composition of alexandrite and being a natural sample. It was possible to observe that alexandrite shows potential for use in TL and OSL dosimetry, and our investigation strongly support the position that Fe and Cr ions interfere in the obtained results, generating TL broad bands that suggests the superposition of several peaks. More work is in progress to correlate the Cr and Fe concentration and to determine the charge carrier responsible for the TL bands. Also, we can conclude that the content of other impurities play an important role in this process, as the case of Ca that may be related to the defect responsible for low temperature TL peak. A study of alexandrite OSL curves was performed for the first time and more studies are being developed to reach a better understanding of the OSL process. A more detailed characterization of a larger number of samples and different regions of Brazil is being investigated.

ACKNOWLEDGMENTS

Funding for this work was provided by Brazilian agencies São Paulo Research Foundation (FAPESP), grants #2010/16437-0, and National Council for Scientific and Technological Development (CNPq). The authors are grateful Ph.D. Roseli F. Gennari (USP) for use of the OA technique and Ph.D. Marcia Rizzuto for use of the XRF technique.

REFERENCES

Bukin, G.V., Volkov, S.Y. and Matrosov, V.N. 1978. Optical generation in alexandrite ($BeAl_2O_4$:Cr^{3+}). Kvant Tovaya Electronika, 5, 1168 – 1169.

Collins, S.C., Wilkerson, T.D., Wilckwar, V.B., Rees, D., Walling, J.C. and Heller, D.F. 1997. The alexandrite ring laser: A spectrally narrow lidar light source for atmospheric fluorescence and absorption observations. Advances in Atmospheric Remote Sensing with Lidar. Berlin: Springer Verlag, 577-580. http://dx.doi.org/10.1007/978-3-642-60612-0_140.

Escobar-Alarcón, E., Villagrán, E., Camps, E., Romero, S., Villarreal-Barajas, J.E., Gonzáles, P.R. 2003. Thermoluminescence of aluminum oxide thin films subject to ultraviolet irradiation. Thin Solid Films, 433, 126-130.

Ferraz, G.M., Watanabe, S., Souza, S.O., Scalvi, R.M.F. 2002. TL, EPR and Optical Absorption studies on natural alexandrite compared to natural chrysoberyl. Radiation Protection Dosimetry, 100, 471-474.

Groppo, D.P., Caldas, L.V.E. 2014. Luminescent response from BeO exposed to alpha, beta and X radiations. Radiation Measurements, 71, 81-85. http://dx.doi.org/10.1016/j.radmeas.2014.07.009.

Gubelin, E. 1976. Alexandrite from Lake Manyara, Tanzania. Gems&Gemology, 15, 203-209.

Ibrahimi, O.A., Avram, M.M., Hankes, C.W., Kilmer, S.L. and Anderson, R.R. (2011) Laser hair removal. Dermatologic Therapy, 24, 94-107. http://dx.doi.org/10.1111/j.1529-8019.2010.01382.x.

Jacobsohn, L. G.; Roy, A. L.; Mcpherson, C. L.; Kucera, C. J.; Oliveira, L. C.; Yukihara, E. G.; Ballato, J. 2013. Rare earth-doped nanocrystalline MgF_2: Synthesis, luminescence and thermoluminescence. Optical Materials, 35, 2461-2464.

Kim, Y.K., Kim, D.-Y., Lee, S.J., Chung, W.S. and Cho, S.B. 2014. Therapeutic efficacy of long-pulsed 755-nm alexandrite laser for seborrheic keratoses. Journal of the European Academy of Dermatology and Venereology, 28, 1007-1011. http://dx.doi.org/10.1111/jdv.12231.

Lapraz, D., Iacconi, P., Daviller, D., Guilhot, B. 1991. Thermostimulated luminescence and fluorescence of α-Al_2O_3: Cr^{3+} samples (ruby). Physica Status Solidi (a), 126, 521-531.

Li, Y., Tong, X., Yang, J., Yang, L., Tao, J. and Tu, Y. 2012. Q-switched alexandrite laser treatment of facial and labial lentigines associated with Peutz-Jeghers syndrome. Photodermatology, Photoimmunology & Photomedicine, 28, 196-199. http://dx.doi.org/10.1111/j.1600-0781.2012.00672.x.

Liu, Q., Yang, Q.H., Zhao, G.G., Lu, S.Z., Zhang, H.J. 2013. The thermoluminescence and optically stimulated luminescence properties of Cr-doped alpha alumina transparent ceramics. Journal of Alloys and Compounds, 579, 259-262. http://dx.doi.org/10.1016/j.jallcom.2013.06.070.

Mckeever, S.W.S. 1985. Thermoluminescence os Solids, Cambridge, England, Cambridge University Press.

Mckeever, S.W.S. 2001. Optically stimulated luminescence dosimetry. Nuclear Instruments and Methods in Physics Research B, 184, 29-54.

Mckeever, S.W.S. 2011. Optically stimulated luminescence: A brief overview. Radiation Measurements, 46, 1336-1341.

Mittani, J.C.R., Watanabe, S., Chubaci, J.F.D., Matsuoka, M., Baptista, D.L., Zawislak, F.C. 2002. Nuclear Instruments and Methods in Physics Research B, 191, 281-284.

Nilforoushzadeh, M.A., Naieni, F.F., Siadat, A.H. and Rad, L. 2011. Comparation between sequentional treatment with diode and alexandrite lasers versus alexandrite laser alone in the treatment of hirsutism. Journal of Drugs in Dermatology, 10, 1255-1259.

Ollier, N., Fuchs, Y., Olivier, C., Horn, A.H. and Rossano, S. 2015. Influence of impurities on Cr^{3+} luminescence properties in Brazilian esmerald and alexandrite. European Journal of Mineralogy, 27, 783-792. http://dx.doi.org/10.1127/ejm/2015/0027-2484.

Pokorny, P., Ibarra, A. 1993. On the origin of the thermoluminescence of Al_2O_3: Cr, Ni. Journal of Physics: Condensed Matter, 5, 7387-7396.

Pokorny, P., Ibarra, A. 1994. Impurity effects on the thermoluminescence of Al_2O_3. Journal of Applied Physics, 75 (2), 1088-1092.

Powell, R.C., Xi, L., Gang, X., Quarles, G.J. and Walling, J.C. 1985. Spectroscopy properties of alexandrite crystals. Physical Review B, 32, 2788 – 2797.

Rabadanov, M.K. and Dudka, A.P. 1997. Comparative structural study of Al2BeO4 and Al_2BeO_4:Cr^{3+} . Inorganic Materials, 33, 48 – 51.

Rocha, M.S.F., Pontuschka, W.M., Verzini, R., Blak, A.R. 2003. Radiation-induced defects in calcium aluminate glasses. Radiation Effects & Defects in Solids, 158, 363-368. http://dx.doi.org/10.1080/104015021000052999.

Rossi, M., Dell´Aglio, M., Giacomo, A., Gaudiuso, R., Senesi, G.S., Pascale, O., Capitelli, F., Nestola, F. and Ghiara, M.R. 2014. Multi-methodological investigation of kunzite, hiddenite, alexandrite, elbaite and topaz, based on laser-induced breakdown spectroscopy and conventional analytical techniques for supporting mineralogical characterization. Physics and Chemistry of Minerals, 41, 127–140. http://dx.doi.org/10.1007/s00269-013-0631-3.

Saedi, N., Metelitsa, A., Petrell, K., Arndt, K.A. and Dover, J.S. 2012. Treatment of tattoos with a picosecond alexandrite laser. Arch Dermalogy, 148, 1360-1363. http://dx.doi.org/10.1001/archdermatol.2012.2894.

Salah, N., Khan, Z.H., Habib, S.S. 2011. Nanoparticles of Al_2O_3: Cr as a sensitive thermoluminescent material for high exposures of gamma rays irradiations. Nuclear Instruments and Methods in Physics Research B, 269, 401-404. http://dx.doi.org/10.1016/j.nimb.2010.12.054.

Scalvi, R.M.F., Ruggiero, L.O. and Siu Li, M. 2002. Influence of annealing on X-ray diffraction of natural alexandrite. Powder Diffraction, 17, 135-138. http://dx.doi.org/10.1154/1.1428284.

Scalvi, R.M.F., Siu Li, M. and Scalvi, L.V.A. 2005. Thermal annealing-induced electric dipole relaxation in natural alexandrite. Physical and Chemistry of Minerals, 31, 733-737. http://dx.doi.org/10.1007/s00269-004-0442-7.

Suchocki, A.B., Gilliland, G.D., Powell, R.C., Bowen, J.M. and Walling, J.C. 1987 Spectroscopy properties of alexandrite crystals II. Journal of Luminescence, 37, 29-37. http://dx.doi.org/0.1016/0022-2313(87)90179-7.

Toosi, S., Ehsani, A.H., Noormohammadpoor, P., Esmaili, N., Mirshams-Shahshahani and Moineddin, F. 2010. Journal of the European Academy of Dermatology and Venereology, 24, 470-473. http://dx.doi.org/10.1111/j.1468-3083.2009.03448.x.

Torezan, L.A.R. and Osório, N. 1990. Laser em Dermatologia: princípios físicos, tipos e indicações. Brazilian Annals of Dermatology, 74, 13 – 20.

Trindade, N.M., Blak, A.R., Yoshimura, E.M., de Andrade Scalvi, L.V. and Scalvi, R.M.F. 2016. Photo-Induced Thermally Stimulated Depolarization Current (TSDC) in Natural and Synthetic Alexandrite ($BeAl_2O_4$:Cr^{3+}). Materials Sciences and Applications, 7, 881-894. http://dx.doi.org/10.4236/msa.2016.712067.

Trindade, N.M., Scalvi, R.M.F. and Scalvi, L.V.A. 2010. Cr^{3+} distribuiton in Al_1 and Al_2 sites of alexandrite ($BeAl_2O_4$:Cr^{3+}) induced by annealing, investigated by optical spectroscopy. Energy and Power Engineering, 2010, 18-24. http://dx.doi.org/10.4236/epe.2010.21004.

Villarreal-Barajas, J.E. Escobar-Alarcón, L., González, P.R., Camps, E., Barboza-Flores, M. 2002. Thermoluminescence properties of aluminum oxide thin films obtained by pulsed laser deposition. Radiation Measurements, 35, 355-359.

Wang, Y., Qian, H. and Lu, Z. 2012. Treatment of café au lait macules in Chinese patients with a Q-switched 755-nm alexandrite laser. Journal of Dermatological Treatment, 23, 431-436. http://dx.doi.org/10.3109/09546634.2011.590790.

Weber, S.U., Grodzicki, M., Lottermoser, W., Redhammer, G.J., Tippelt, G., Ponahlo, J. and Amthauer, G. 2007. ^{57}Fe Mossbauer spectroscopy, X-ray single-crystal diffractometry, and electronic structure calculations on natural alexandrite. Physics and Chemistry of Minerals, 34, 507-515. http://dx.doi.org/10.1007/s00269-007-0166-6.

Yarovoi, P.N., Medvedev, V.Ya., Bukin, G. V., Ivanova, L. A., Mikhalenko, A. A. 1991. Radiative Creation of Color Centers in Alexandrite Crystals. Opt. Spectrosc. (USSR) 71(5), 447–449.

Yoshimura, E.M. 2007. Correlation of optically stimulated luminescence and thermoluminescence of Al_2O_3: Fe, Mg, Cr crystals. Nuclear Instruments and Methods in Physics Research A, 580, 606-609. http://dx.doi.org/10.1016/j.nima.2007.05.021.

Yoshimura, E.M., Yukihara, E.G. 2006. Optically stimulated luminescence: searching for nex dosimetric materials. Nuclear Instruments and Methods in Physics Research B, 250, 337-341. http://dx.doi.org/10.1016/j.nimb.2006.04.134.

Yukihara, E. G.; Mckeever, S. W. S. 2011. Optically Stimulated Luminescence: Fundamentals and Applications. West Sussex, UK: John Wiley and Sons, Ltd.

Yukihara, E.G. 2001. Desvendando a Cor e Termoluminescência do Topázio: Um Estudo dos Defeitos e Processos Termicamente e Opticamente Estimulados no Cristal Natural (portuguese). Thesis, USP, São Paulo.

Materials Sciences and Applications, 2016, 7, 881-894
http://www.scirp.org/journal/msa
ISSN Online: 2153-1188
ISSN Print: 2153-117X

Photo-Induced Thermally Stimulated Depolarization Current (TSDC) in Natural and Synthetic Alexandrite ($BeAl_2O_4:Cr^{3+}$)

Neilo Marcos Trindade[1,2], Ana Regina Blak[1], Elisabeth Mateus Yoshimura[1], Luis Vicente de Andrade Scalvi[3], Rosa Maria Fernandes Scalvi[3]

[1]São Paulo Federal Institute, São Paulo, Brazil
[2]Institute of Physics, University of São Paulo, São Paulo, Brazil
[3]Department of Physics, São Paulo State University, Bauru, Brazil
Email: ntrindade@ifsp.edu.br

How to cite this paper: Trindade, N.M., Blak, A.R., Yoshimura, E.M., de Andrade Scalvi, L.V. and Scalvi, R.M.F. (2016) Photo-Induced Thermally Stimulated Depolarization Current (TSDC) in Natural and Synthetic Alexandrite ($BeAl_2O_4:Cr^{3+}$). *Materials Sciences and Applications*, **7**, 881-894.
http://dx.doi.org/10.4236/msa.2016.712067

Received: November 16, 2016
Accepted: December 11, 2016
Published: December 14, 2016

Abstract

The investigation of electrical properties in alexandrite ($BeAl_2O_4:Cr^{3+}$) in synthetic and natural forms is presented in this paper. Alexandrite is a rare and precious mineral that changes color according to the light incident on it. In the synthetic form, it is used technologically as an active laser medium. The electrical characterization was obtained using the Thermally Stimulated Depolarization Current (TSDC) technique, an interesting tool to study the behavior of impurities in insulators. Alexandrite presented the electric dipole relaxation phenomenon, both in natural and in synthetic samples. It was possible to observe TSDC bands for the synthetic sample at around 170 K, and at around 175 K for the natural sample. Besides, photo-induced TSDC measurements were performed through the excitement of the samples by using a continuous wave argon laser. In addition, photoluminescence measurements were performed to verify in advance whether the laser light would be absorbed by the sample, and in order to complement the photo-induced TSDC measurements analysis. The results of photo-induced TSDC experiments have contributed to the understanding of the TSDC bands behavior: the results obtained with the technique suggest that there is an effective participation of Cr^{3+} ions in the formation of TSDC bands because they were more intense when the sample was exposed to the argon laser beam.

Keywords

Alexandrite, Chrysoberyl, Thermally Stimulated Depolarization Current (TSDC), Photoluminescence, Photo-Induced

1. Introduction

Alexandrite is a variety of chrysoberyl crystal that contains chromium in its structure and presents the following chemical composition: $BeAl_2O_4:Cr^{3+}$ [1] [2]. Brazil is one of the largest producers of natural alexandrite [2]; it belongs to families of gems of high economical and technological interest [3].

The technological importance of alexandrite has increased after 1974, when it was possible to use it in synthetic form as an active laser medium, with superior characteristics when compared to other types of media, with emission in the range between 700 and 800 nm [4]. The first scientists who suggested the possibility of application of synthetic alexandrite as laser crystals were Farrel in 1963 [5], but they were not successful in obtaining it in practice [6]. Bukin *et al.* first reported the alexandrite laser in 1978 [7]. The Q-switched alexandrite laser operates in the range of 755 nm, near infrared emission spectrum. Its pulse lasts about 100 ns, and its long wavelength allows deep penetration into the skin [8], so it is widely used in dermatology, as well as other popular lasers such as the Q-switched ruby (QSR) (694 nm) and Q-switched Nd:YAG laser (1064 nm and 532). There are many recent works showing applications of the alexandrite laser in medicine as in the treatment of facial and labial lentigines associated with Peutz-Jeghers syndrome [9], café au lait macules [10], seborrheic keratoses [11], hirsutism [12], trichostasis spinulosa [13] and other applications such as hair removal [14] and tattoos removal [15].

An important property is its color change according to light incident on it. If exposed to incandescent light, rich in red wavelengths, alexandrite has a red color. Exposing alexandrite to natural light, with a smaller portion in the red region of the spectrum, it generates shades of dominant blue-green color. This phenomenon is referred in the literature as alexandrite effect [16] [17]. The color change results in popularity and high market value of alexandrite as a gem. Furthermore, the alexandrite crystal is mechanically rigid and provides good thermal conductivity [18].

Figure 1 shows chrysoberyl structure. In chrysoberyl the unit cell contains four molecules with eight Al^{3+} ions (ionic radius 0.535 Å) occupying distorted octahedral sites, and four Be^{2+} ions (0.47 Å) occupying distorted tetrahedral sites formed with oxygen ions located in planes perpendicular to the c-axis [19]. Due to the small ionic radius of

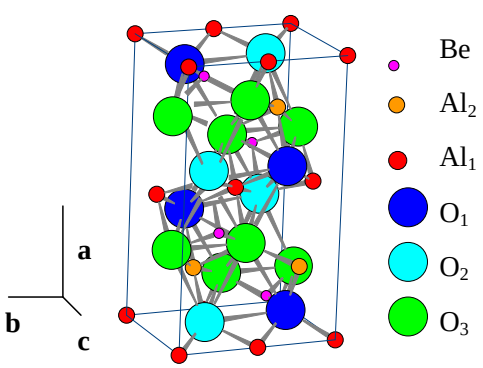

Figure 1. Chrysoberyl structure [4] [18].

Be^{2+}, the crystal structure of chrysoberyl has a lower symmetry than the spinel mineral group with similar chemical formulas [20]. Such ionic radius also results in a bond length in the Be-O of 1.637 Å [17]. Two of the three oxygen positions are located in a reflection plane and the third oxygen occupies a general position [20]. The chrysoberyl crystallization has an orthorhombic structure that corresponds to dense hexagonal packing, influencing the oxygen atom (atomic radius 2.7 Å) positions, which are slightly distorted by the presence of aluminum atoms. These distortions caused by aluminum give rise to two sites of different symmetries: a site, Al_1, set in an inversion center (Ci symmetry) and a site, Al_2, located in a reflection plane (Cs symmetry) [22] [23].

In two sites of different symmetries the Al^{3+} ions are replaced by Cr^{3+} (0.615 Å) generating alexandrite. The larger site, named Al_2, is preferably occupied by Cr^{3+} ions [18]. The octahedron containing Al_2 sites, is regarded as larger than the Al_1 octahedron, because the Al-O bond length (1.938 Å) is wider at that site than at Al_1 (1.890 Å), resulting in a larger volume polyhedron [17]. According to literature, Cr^{3+} ions located in Al_2 sites are responsible for the optical properties of alexandrite, including laser emission [24].

The electrical properties studied here can contribute to the understanding of the optical properties observed in alexandrite, such as the impurities aggregated in this crystal having diverse charge states.

2. Materials and Methods

The synthetic sample has been grown by H. P. Jenssen and R. Morris (from Allied Signal Inc., USA), by the Czochralski method [25]. Iridium crucibles, zirconia ceramic furnaces and $N_2^-O_2$ atmospheres were used, obtaining the following result: [001] oriented blades measuring about 1 cm × 2 cm with Cr^{3+} substitutions of up to 0.3% atm (of $A1^{3+}$ sites) [26]. The sample faces were perfectly paralleled, with thickness of 2.33 mm. Alexandrite rock pieces come from Minas Gerais state, Brazil, and show a dark green color. Samples have been cut in small pieces with thickness of 1.5 mm.

The optical studies and electrical characterization of alexandrite can significantly contribute to the technological application of the material. The Thermally Stimulated Depolarization Currents (TSDC) technique successfully allows the understanding of the electric dipole relaxation mechanisms present in minerals [4] [27] [28] [29] [30] [31]. In addition, the TSDC technique can also be used in a modified manner, when the sample is photo-excited along with the electric field and then the effects on the material are analyzed.

Through one single measurement, the TSDC technique represents a very sensitive and accurate method for the determination of physical parameters such as relaxation time (τ), activation energy (E_a) and dipole moment strength (p) associated with defects with dipolar characteristics. Electric dipole characteristics are one of the requirements to detect the behavior of defects in solids using this technique [32]. The TSDC method consists of four basic steps: the sample is first polarized in an electric field E_p for a time t_p, at temperature T_p. This temperature should be such that the dipoles can still be sta-

tistically oriented with the electric field applied in a certain time t_1, and should not be so high that heavy space charge contributes to the signal. To ensure good polarization, dipoles must be polarized by a time $t_P \gg \tau(T_P)$. Then, in the second step, the temperature of the sample is reduced to $T_o \ll T_p$ so that the dipole relaxation time is long enough to prevent movements at low temperatures. At this stage, it can be said that the dipoles are "frozen" and statistically aligned with the applied field. After reaching T_o (the liquid nitrogen temperature, in our experiment) the field is removed and an electrometer is connected to the sample (third step). After the initial capacitive discharge in the sample, it is heated at a constant rate $b = dT/dt$, and the current is recorded as a function of temperature in the final step of TSDC. The relaxation times become short and a current depolarization $i(T)$ is detected when the dipoles lose their preferential polarization orientation. During the time in which this process occurs, the current first increases exponentially, and continues increasing until a maximum value is reached; and then falls rapidly as Figure 2 illustrates. The physical process of TSDC measurement and behavior of dipoles presented in each step of the technique are also in Figure 2.

Previous to the measurement, the faces of the samples in contact with the electrodes are painted with silver paint to improve electrical contact for the application of electric field. The sample is polarized initially at room temperature and, after a first step to identify the TSDC peaks, the polarization is made near the peak of TSDC and an electric field is applied for a predetermined period of time in order to reduce the lattice contributions. After that time, the cryostat walls are put in contact with liquid nitrogen to produce a rapid temperature decrease. When the sample reaches a temperature of approximately 77 K, the electric field is turned off. The same terminal is connected to an electrometer that will measure the depolarization current. When the current is stabilized, the sample is heated at 6 K/min, up to 300 K. The polarization electric field is about 1.4 kV/mm value that considers the thickness of the sample.

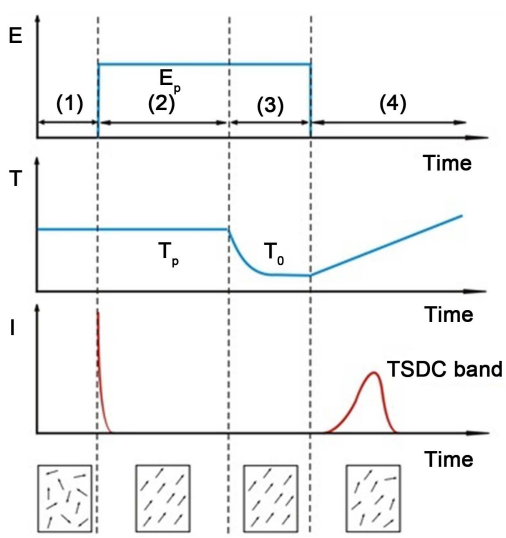

Figure 2. Physical process of TSDC measurements and behavior of dipoles.

In measurements of photo-induced TSDC, the process is quite similar to the TSDC one. The scheme and steps of this method are shown in Figure 3. We have used two different methodologies to illuminate the sample, as explained next.

In the first process (i), in Figure 3, after the application of the electric field at a given polarization temperature (2), the temperature is decreased rapidly to a temperature close to 77 K (3). After removing the applied electric field, a laser beam is shined on the sample for a given time (4). The laser beam is removed and the temperature is increased at a constant rate, as usual. In this case, it is considered that the dipoles are already oriented and "frozen" when the laser is applied –we investigate the possible effect in this polarization direction with the incidence of laser beam in the material. In the second case (ii), in Figure 3, when the sample reaches a temperature close to 77 K (2), the electric field is applied together with the laser beam, but for different intervals (3) and (4). After removing the laser beam, the temperature is increased at a constant rate. In this case, it is considered that the dipoles are randomly oriented because they had not yet been "frozen" without the application of a previously bias field. This way, we seek to investigate the effect on these dipoles and if their orientation in these same conditions is possible with the absorption of photons of the laser beam.

The TSDC equipment makes use of a Janis Research VPF-100 model cryostat provided with transparent windows, high voltage source Keithley 248 High Voltage Supply model, a Lakeshore 321 temperature controller model, an electrometer Keithley 6517A model and a turbomolecular pump system Boc Edwards GI, 70H/E2M1.5/Ticcart model. The measurements were made using an automatic acquisition system data, the USB-6008 board 12-bit, 10 kS/s Multifunction I/O and NI-DAQmx software. To carry out the photo-induced TSDC measurements, an argon laser was used with beam di-

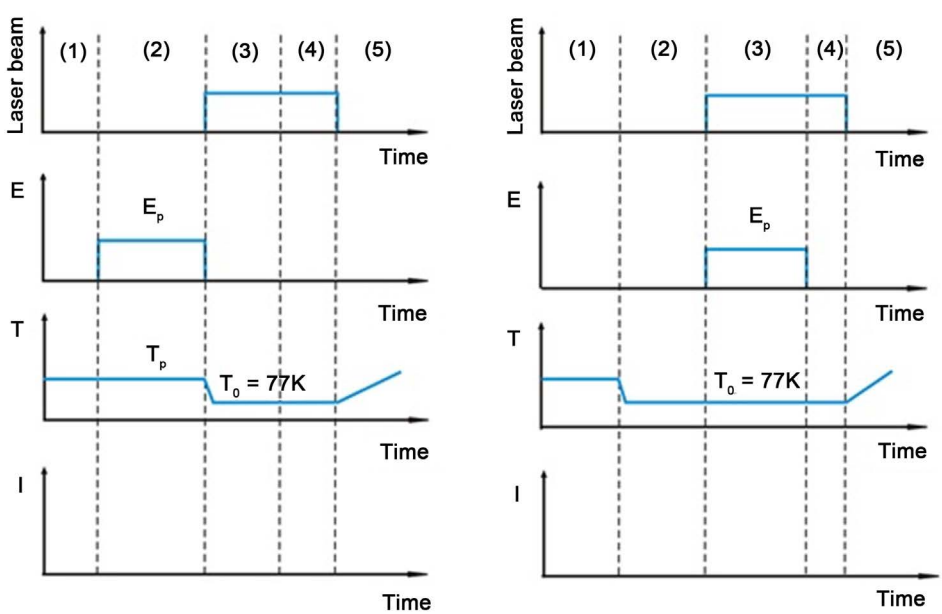

Figure 3. Scheme of photo-induced TSDC measurements, indicating the methods used: process i and process ii.

rected to the sample by means of lenses and mirrors. Chemical analyses were performed using Scanning Electronic Microscopy (SEM), the Energy Dispersive (EDS) and Spectroscopy Wavelength Dispersive (WDS) techniques. The Argon laser emissions (Spectra 2017 model), with energy hν = 2.51 eV, were used in the photoluminescence excitation and TSDC measurements. The light emitted by the sample is sent to the spectrometer and then to a detector due to the energy region where the measurement was made. The entire system is connected to a computer that controls the spectrometer and processes the data.

3. Results and Discussion

3.1. Chemical Analysis

Table 1 shows the results of two techniques (EDS and WDS) used to obtain the concentration of iron, aluminum and chromium contained in the sample. Both the techniques do not detect Be element due to its atomic number (smaller than 8).

The environment, the temperature and other important parameters of the natural materials forming process also influence the various types of impurities which may be incorporated in bulk rock, such as K, Si and Ca. The Table 1 results show that iron concentration is substantially larger compared to chromium. Moreover, iron can also be related to the color of alexandrite [17]. It is of great importance to highlight the presence of Fe, which is verified due to the presence of inclusions in natural alexandrite. According to Weber *et al.* [17], based on chemical and geometric arguments, it is assumed that, in alexandrite originated from Russia, the Fe^{3+} ion replaces Al in octahedral sites in the structure once the tetrahedron Be site is too small for such replacement. It can also occur the replacement of Al^{3+} to Fe^{2+} with the locally distorted octahedral coordination and expanded in accordance with the large ionic radius of Fe^{2+} (0.750 Å) compared with Al^{3+} (0.535 Å). Thus, the charge is compensated by the presence of Ti tetravalent in the alexandrite. Both bivalent and trivalent iron in different Al positions has a certain preference for the wider site, Al_2. Furthermore, a refinement of the structure shows that most of the iron is trivalent, but a small amount of bivalent iron is also detected, and that the incorporation of iron occurs in Al sites. In the TSDC measurements, Fe bands are observed only in natural samples.

The Cr^{3+} ions in Al_2 are responsible for the laser property and characterize the high probability of electric dipole transitions. The transitions in the magnetic dipole type Cr^{3+} ions in Al_1 do not significantly contribute to the photoluminescence of the material and, furthermore, are excluded from the laser process, as well as reinforcing the non-

Table 1. Composition of natural alexandrite obtained through EDS and WDS analysis.

Element	EDS (%WT)	WDS (%WT)
Al	76.45	-
Cr	0.09	0.13
Fe	0.44	0.61

radiative processes, degrading the efficiency of the laser [6] [33]. For the photo-induced electrical characterization it is necessary to verify that the material shows luminescence in the same temperatures that occur polarization.

3.2. Photoluminescence

In the luminescence spectrum, the Cr^{3+} ions lines in Al_2 are called R_1 and R_2, and the Cr^{3+} ions lines in Al_1 are called S_1 and S_2. Figure 4 shows the separation of R and S lines both for the natural and synthetic samples. As experimentally verified and presented in literature [34] [35], R_1 and R_2 lines appear in precisely the same wavelength at 680.4 nm and 678.5 nm, respectively, in both spectra, absorption and emission at room temperature and are associated with transitions from the ground state to the ^2E level. In the emission spectrum, the lines S_1 and S_2 appear at 695.8 and 689.9 nm positions as well as in the optical absorption as narrow lines at 655.7, 649.3 and 645.2 nm.

Figure 4 shows the luminescence spectrum for synthetic and natural samples whose transitions in the reflection site (R lines) are around 680 nm and 678.5 nm, in the inversion site (S lines) are around 695.5 nm and 690 nm. The R line is assigned to the forbidden $^2E \rightarrow {}^4A_2$ transition of Cr^{3+} [3]. The R lines in the emission spectrum are more intense than the S lines because the spectrum is dominated by the transitions associated with Cr^{3+} ions in Al_2 compared to Cr^{3+} ions in Al_1 [3] [23] [35]. This result was clearly observed for the natural sample.

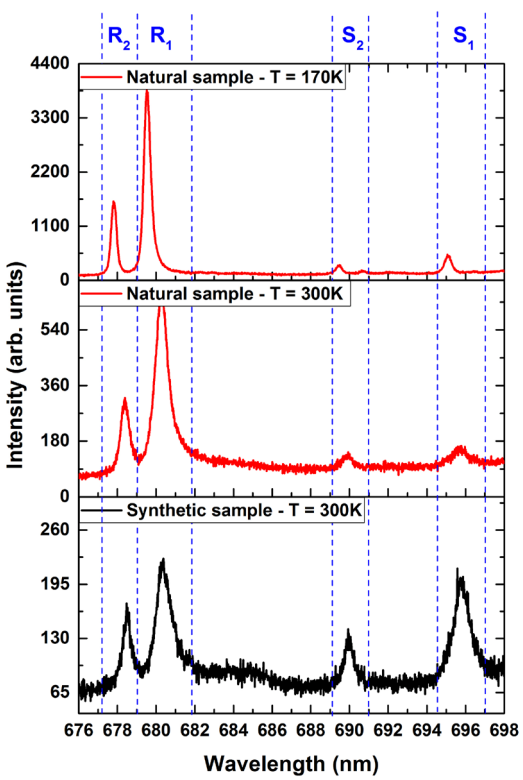

Figure 4. Photoluminescence spectrum of synthetic and natural alexandrite with exposure to argon laser (488 nm).

3.3. Photo-Induced Thermally Stimulated Depolarization Current

Assuming that the source of the dipole is essentially the participation of Cr^{3+} ions, it is interesting to analyze the results of photo-induced TSDC measurements because these ions are responsible for emission lines in the photoluminescence spectra, and thus, we seek to investigate a photo-excited influence on the bands of TSDC. Regarding to electrical properties, according to the literature [4], the possible formation of dipoles in alexandrite is related to its crystalline structure. The structure has the Al_1 and Al_2 linked sites, each one with six oxygen atoms, three of which are independent and symmetrically designated O_1, O_2 and O_3. The simple aforementioned replacement of Cr^{3+} to Al^{3+} in the structure would be able to cause the formation of dipoles. Nevertheless, the difference between the ionic radius Al^{3+} (0.535 Å) and Cr^{3+} (0.615 Å) in alexandrite can trigger the dipoles. It is also likely that the presence of oxygen vacancies leads to the presence of dipoles of impurity-vacancy type caused by different distances between Cr^{3+} and vacancy. One last possibility is the presence of other structure intrinsic defects, especially in the case of natural samples. The TSDC measurements were taken with a synthetic and a natural sample.

In photo-induced TSDC we used a high quality synthetic sample. The sample had already been polished and its faces parallel to each other, through which the electric field is applied. The sample was polarized for 7 minutes at room temperature with a 3300 V. We chose to carry out the process (i), photo-induced TSDC. The measurement was repeated twice with exposure to argon laser, for equal periods of time, but with different powers, as shown in Figure 5.

In Figure 5, TSDC curve for synthetic sample shows a broad band with maximum intensity around 170 K. We believe that above 230 K the results are not related to the effects of dipolar relaxation. It is likely that bands at these temperatures are due to a

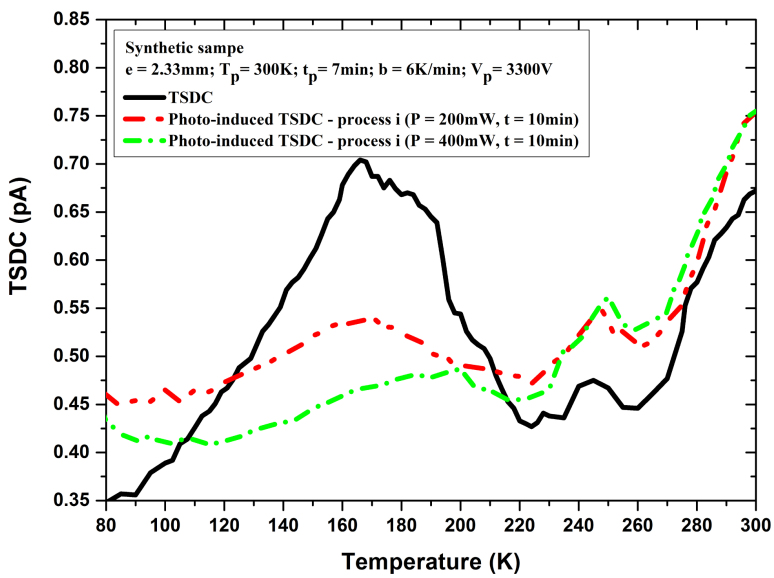

Figure 5. TSDC and photo-induced TSDC data for a synthetic sample, with exposure to argon laser (488 nm), in process i.

contact effect. It can be concluded from Figure 5 that the increase in the laser power, leads to the process of "destruction" of dipoles, as be the main band has a decreased area, which is the quantity related to the number of oriented dipoles. To that extent, it is also clear that the dipolar relaxation can occur by photo-excitation, and not only by a thermal process, which is also a process dependent on the power of the laser used.

In the case of a natural sample, it is important to determine the dependence of the relaxation dipolar process with the electric field the TSDC measurement. It was performed for four different values, 800 V, 1000 V, 1200 V and 1400 V, shown in Figure 6.

In Figure 6, for natural sample, it can be seen that the area under the TSDC curve is proportional to the applied field, according to the picture inserted. The graph is consistent with the dipolar relaxation theory, with increasing voltage applied, there are an increased number of dipole relaxations, and, in turn, curves become more defined and the maximum intensity of current increases.

As for the synthetic sample, polarization was carried out similarly in natural samples, including the length of polarization time. Nevertheless, a 1400 V voltage value was applied in accordance with its thickness. In addition to analyze the consequences of photo-excitation, the photo-induced TSDC, process i and ii were performed. Figure 7 shows obtained result.

The photo-induced TSDC results, for same natural sample, it can be seen in Figure 7. In process i (Figure 3), an intense band with its maximum at around 175 K is observed.

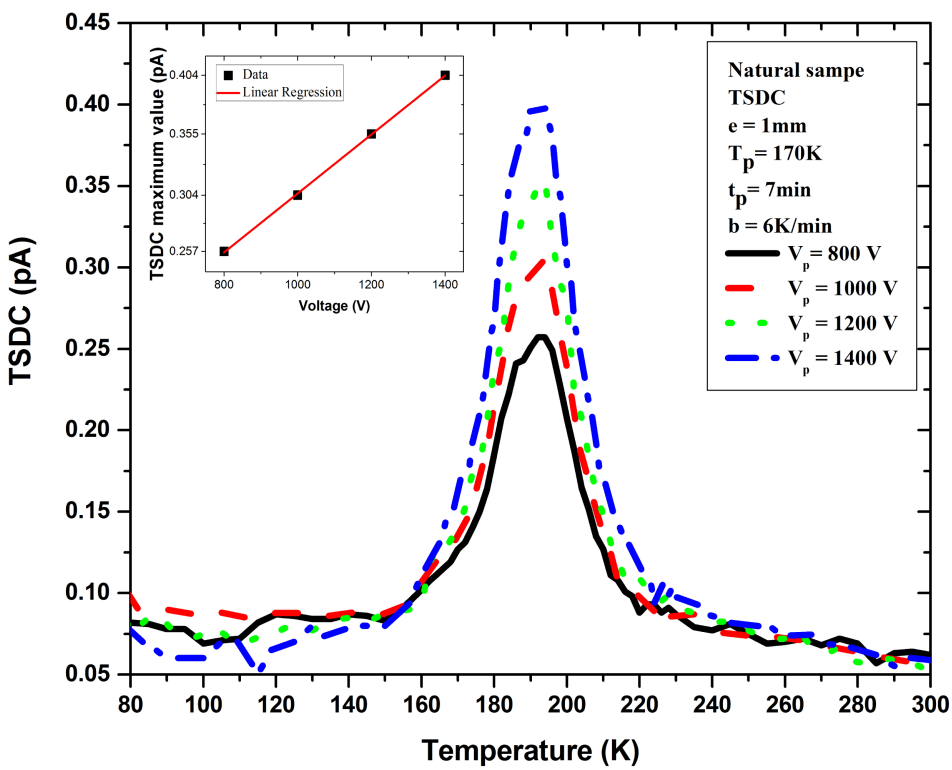

Figure 6. TSDC data for a natural sample, with application of four different voltages. The inset shows the linear dependence of TSDC maximum peak intensities with applied voltage.

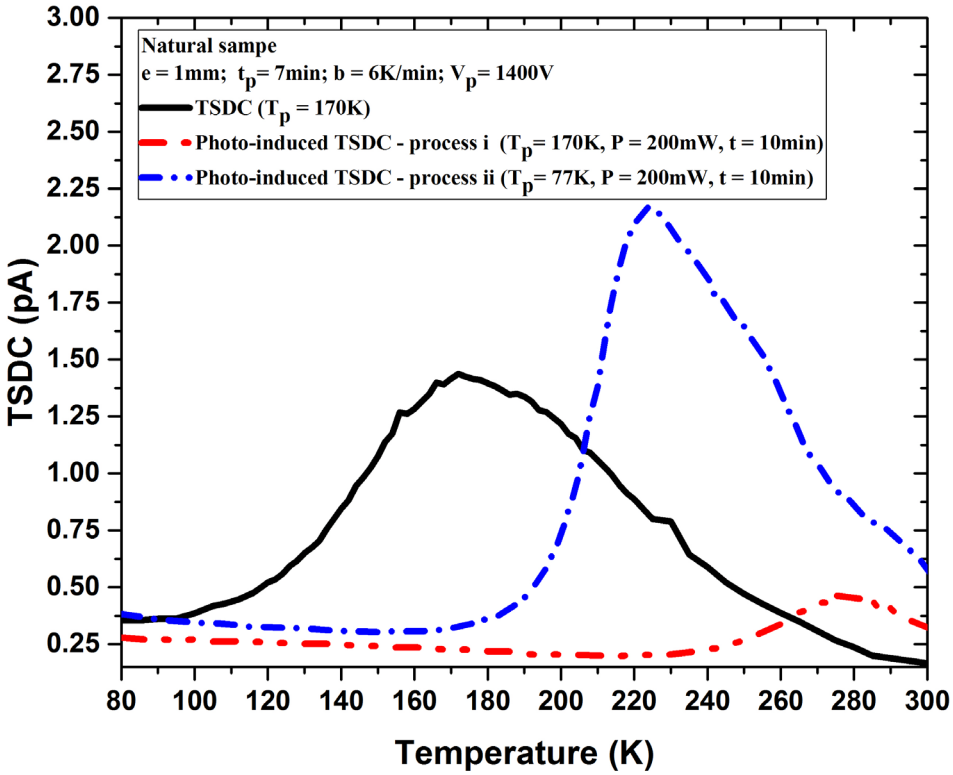

Figure 7. TSDC and photo-induced TSDC data for a natural sample, with exposure to argon laser (488 nm), in processes i and ii.

A comparison can be drawn between the power required to destroy the TSDC band in a natural and in a synthetic sample. The natural sample band at around 175 K disappears even with lower laser power (200 mW), whereas, the synthetic sample requires a larger power to do so. The process ii (**Figure 3**) was carried out using the same conditions, it is observed that this method promotes TSDC band for this sample with an intense band around 230 K. We are convinced that this orientation of dipoles in low temperature (77 K) by the laser light is possible, because of the synergism of the photon energies of the laser beams together with the applied electric field. Interestingly, it can be seen in these results that TSDC bands for natural samples are better defined and more intense at the maximum temperature than for synthetic samples. To understand these results, one should consider that in the natural samples there is presence of Fe^{3+} ions observed in optical absorption measurements in the spectral region of ultraviolet, and other additions such as OH and SiO_4 can be seen in optical absorption measurements in the spectral infrared region [2]. These inclusions may lead to dipolar relaxation in the same temperature region, which is a Cr^{3+} and vacancy characteristic. Consequently, the TSDC band for these natural samples can be observed as a superposition of other bands of TSDC.

Regarding photo-induced measurements, it was observed that the process of destruction of TSDC bands in natural sample occurs more noticeably than in the synthetic one, which has dependence on the power of the applied laser. This result is in agreement

with previous work [36] when it done to synthetic samples, and should contribute to the interpretation of results in natural samples presented in the literature. Also according to these authors, it is suggested that this process of destruction of TSDC bands does not occur for natural samples for they have irregular faces causing scattering of the light incident on it. Nonetheless, this work presents unprecedented results of destruction of bands in such samples. A small band around 280 K was also observed, which apparently is not influenced by laser presence and may be associated with contact effect.

4. Conclusions

The present work demonstrates that the material presents electric dipole relaxation phenomenon, both in natural and in synthetic samples. In this study, it was assumed that Cr^{3+} ions form dipole defects in the material. Chemical analysis of natural samples showed a large concentration of Fe in the material, predicted to be present in the Al_2 site, which can interfere in the obtained results.

It was possible to observe TSDC bands for synthetic sample, around 170 K, and around 175 K in natural sample. The TSDC experiment was performed with modification using an argon laser source, method called photo-induced TSDC. It was observed in the results that when the (i) process is carried out, the destruction of the TSDC band occurs in synthetic and natural samples. That way, you can disorient the dipoles at low temperature (77 K) and, consequently, most likely destroy TSDC bands at the temperature they occur, and to the synthetic sample it was found that there is a laser power dependence on the effective destruction of these bands. The result of the (ii) process shows that the incidence of the laser beam provides a more effective orientation of dipoles and, consequently, an increase in the intensity of TSDC band if compared to the situation without laser beam in natural samples.

These results of photo-induced TSDC suggest that there is an effective participation of Cr^{3+} ions in the formation of TSDC bands. This statement comes from the correlation between the measurements of electrical characterization and optical characterization of alexandrite. This is possible because the photoluminescence measurements confirmed the presence of Cr^{3+} emission lines with the incidence of the same laser used in photo-induced measurements. Another interesting fact was that the TSDC bands were more intense when the sample was exposed to the laser beam, thus promoting greater orientation of dipoles related to the presence of oxygen vacancies associated with Cr^{3+}, and change local load due to substitution of Al^{3+} sites by Cr^{3+} ions.

Future efforts will be directed to thermoluminescence (TL) investigations of natural alexandrite. Thermoluminescence is the thermally stimulated emission originated from energy that was previously stored in the crystal during exposition to ionizing radiation. Initial measurements show that the alexandrite sample exhibits the TL peaks and it is likely that Cr^{3+} ions have an important part in this process.

Acknowledgements

Funding for this work was provided by Brazilian agencies FAPESP, CNPq and CAPES.

The authors are grateful to Prof. Dr. Américo S. Tabata for use of the PL technique facilities and Mr. Luciano B. Ramos for language review.

References

[1] Rossi, M., Dell'Aglio, M., Giacomo, A., Gaudiuso, R., Senesi, G.S., Pascale, O., Capitelli, F., Nestola, F. and Ghiara, M.R. (2014) Multi-methodological Investigation of Kunzite, Hiddenite, Alexandrite, Elbaite and Topaz, Based on Laser-Induced Breakdown Spectroscopy and Conventional Analytical Techniques for Supporting Mineralogical Characterization. *Physics and Chemistry of Minerals*, **41**, 127-140. https://doi.org/10.1007/s00269-013-0631-3

[2] Trindade, N.M., Scalvi, R.M.F. and Scalvi, L.V.A. (2010) Cr^{3+} Distribution in Al_1 and Al_2 Sites of Alexandrite ($BeAl_2O_4$:Cr^{3+}) Induced by Annealing, Investigated by Optical Spectroscopy. *Energy and Power Engineering*, **2010**, 18-24. https://doi.org/10.4236/epe.2010.21004

[3] Ollier, N., Fuchs, Y., Olivier, C., Horn, A.H. and Rossano, S. (2015) Influence of Impurities on Cr^{3+} Luminescence Properties in Brazilian Esmerald and Alexandrite. *European Journal of Mineralogy*, **27**, 783-792. https://doi.org/10.1127/ejm/2015/0027-2484

[4] Scalvi, R.M.F., Siu Li, M. and Scalvi, L.V.A (2005) Thermal Annealing-Induced Electric Dipole Relaxation in Natural Alexandrite. *Physical and Chemistry of Minerals*, **31**, 733-737. https://doi.org/10.1007/s00269-004-0442-7

[5] Farrel, E.F., Fang, J.H. and Newham, H.P. (1963) Refinement of the Chrysoberyl Structure. *American Mineralogist*, **48**, 804-810.

[6] Sevest'yanov, B.K. (2003) Excited-State Absorption Spectroscopy of Crystals Doped with Cr^{3+}, Ti^{3+}, and Nd^{3+} Ions—Review. *Crystallography Reports*, **48**, 989-1011. https://doi.org/10.1134/1.1627442

[7] Bukin, G.V., Volkov, S.Y. and Matrosov, V.N. (1978) Optical Generation in Alexandrite ($BeAl_2O_4$:Cr^{3+}). *Kvanttovaya Electronika*, **5**, 1168-1169.

[8] Torezan, L.A.R. and Osório, N. (1990) Laser in Dermatology: Physical Principles, Types and Indications. *Brazilian Annals of Dermatology*, **74**, 13-20.

[9] Li, Y., Tong, X., Yang, J., Yang, L., Tao, J. and Tu, Y. (2012) Q-Switched Alexandrite Laser Treatment of Facial and Labial Lentigines Associated with Peutz-Jeghers Syndrome. Photodermatology, *Photoimmunology & Photomedicine*, **28**, 196-199. https://doi.org/10.1111/j.1600-0781.2012.00672.x

[10] Wang, Y., Qian, H. and Lu, Z. (2012) Treatment of Café Au Lait Macules in Chinese Patients with a Q-Switched 755-nm Alexandrite Laser. *Journal of Dermatological Treatment*, **23**, 431-436. https://doi.org/10.3109/09546634.2011.590790

[11] Kim, Y.K., Kim, D.-Y., Lee, S.J., Chung, W.S. and Cho, S.B. (2014) Therapeutic Efficacy of Long-Pulsed 755-nm Alexandrite Laser for Seborrheic Keratoses. *Journal of the European Academy of Dermatology and Venereology*, **28**, 1007-1011. https://doi.org/10.1111/jdv.12231

[12] Nilforoushzadeh, M.A., Naieni, F.F., Siadat, A.H. and Rad, L. (2011) Comparation between Sequentional Treatment with Diode and Alexandrite Lasers versus Alexandrite Laser Alone in the Treatment of Hirsutism. *Journal of Drugs in Dermatology*, **10**, 1255-1259.

[13] Toosi, S., Ehsani, A.H., Noormohammadpoor, P., Esmaili, N., Mirshams-Shahshahani, M. and Moineddin, F. (2010) Treatment of Trichostasis Spinulosa with a 755-nm Long-Pulsed Alexandrite Laser. *Journal of the European Academy of Dermatology and Venereology*, **24**, 470-473. https://doi.org/10.1111/j.1468-3083.2009.03448.x

[14] Ibrahimi, O.A., Avram, M.M., Hankes, C.W., Kilmer, S.L. and Anderson, R.R. (2011) Laser Hair Removal. *Dermatologic Therapy*, **24**, 94-107. https://doi.org/10.1111/j.1529-8019.2010.01382.x

[15] Saedi, N., Metelitsa, A., Petrell, K., Arndt, K.A. and Dover, J.S. (2012) Treatment of Tattoos with a Picosecond Alexandrite Laser. *Archives of Dermatology*, **148**, 1360-1363. https://doi.org/10.1001/archdermatol.2012.2894

[16] Gubelin, E. (1976) Alexandrite from Lake Manyara, Tanzania. *Gems & Gemology*, **15**, 203-209.

[17] Weber, S.U., *et al*. (2007) ^{57}Fe Mossbauer Spectroscopy, X-Ray Single-Crystal Diffractometry, and Electronic Structure Calculations on Natural Alexandrite. *Physics and Chemistry of Minerals*, **34**, 507-515. https://doi.org/10.1007/s00269-007-0166-6

[18] Collins, S.C., Wilkerson, T.D., Wilckwar, V.B., Rees, D., Walling, J.C. and Heller, D.F. (1997) The Alexandrite Ring Laser: A Spectrally Narrow Lidar Light Source for Atmospheric Fluorescence and Absorption Observations. In: Ansmann, A., Neuber, R., Rairoux, P. and Wandinger, U., Eds., *Advances in Atmospheric Remote Sensing with Lidar*, Springer Verlag, Berlin, 577-580. https://doi.org/10.1007/978-3-642-60612-0_140

[19] Scalvi, R.M.F., Ruggiero, L.O. and Li, M.S. (2002) Influence of Annealing on X-Ray Diffraction of Natural Alexandrite. *Powder Diffraction*, **17**, 135-138. https://doi.org/10.1154/1.1428284

[20] Ivanov, V.Y., Pustovarov, V.A., Shlygin, E.S., Korotaev, A.V. and Kruzhalov, A.V. (2005) Electronic Excitations in $BeAl_2O_4$, Be_2SiO_4, and $Be_3Al_2Si_6O_{18}$ Crystals. *Physics of the Solid State*, **47**, 466-473. https://doi.org/10.1134/1.1884706

[21] Bauerhansl, P. and Beran, P. (1997) Trace Hydrogen in the Olivine-Type Minerals Chrysoberyl, Al_2BeO_4 and Sinhalite, $MgAlBO_4$—A Polarized FTIR Spectroscopic Study. *Schweizerische Mineralogische und Petrographische Mitteilungen*, **77**, 131-136.

[22] Rabadanov, M.K. and Dudka, A.P. (1997) Comparative Structural Study of Al_2BeO_4 and Al_2BeO_4:Cr^{3+}. *Inorganic Materials*, **33**, 48-51.

[23] Trindade, N.M., Tabata, A., Scalvi, R.M.F. and Scalvi, L.V.A. (2011) Temperature Dependence Luminescence Spectra of Synthetic and Natural Alexandrite ($BeAl_2O_4$:Cr^{3+}). *Materials Science and Applications*, **2**, 284-287. https://doi.org/10.4236/msa.2011.24037

[24] Shepler, K.L. (1984) Fluorescence of Inversion Site Cr^{3+} Ions in Alexandrite. *Journal of Applied Physics*, **56**, 1314-1318. https://doi.org/10.1063/1.334119

[25] Guo, X., *et al*. (1987) Czochralski Growth of Alexandrite Crystals and Investigation of Their Defects. *Journal of Crystal Growth*, **83**, 311-318. https://doi.org/10.1016/0022-0248(87)90292-2

[26] Walling, J.C., Peterson, O.G., Jenssen, H.P., Morris, R.C. and O'Dell, E.W. (1980) Tunable Alexandrite Lasers. *IEEE Journal of Quantum Electronics*, **16**, 1302-1315. https://doi.org/10.1109/JQE.1980.1070430

[27] Cortezão, S.U. and Blak, A.R. (1998) Optical Absorption (OA) and Thermally Stimulated Depolarization Currents (TSDC) in Brazilian Amethyst. *Radiation Effects and Defects in Solids*, **147**, 1-10. https://doi.org/10.1080/10420159808226381

[28] Cortezão, S.U. and Blak, A.R. (2000) Thermally Stimulated Depolarization Currents in Brazilian Amethysts. *Brazilian Journal of Vacuum Applications*, **19**, 43-45.

[29] Cortezão, S.U., Pontuschka, W.M., Rocha, M.S.F. and Blak, A.R. (2003) Depolarisation Currents (TSDC) and Paramagnetic Resonance (EPR) of Iron Amethyst. *Journal of Physics and Chemistry Solids*, **64**, 1151-1155. https://doi.org/10.1016/S0022-3697(03)00043-X

[30] Vismara, M.V.G., Trindade, N.M., Ruggiero, L.O. and Scalvi, R.M.F. (2008) Investigation of

the Phenomenon of Electric Dipolar Relaxation in Brazilian Amethysts. *Brazilian Journal of Vacuum Applications*, **27**, 43-49.

[31] Russo, F.T., Scalvi, R.M.F., Scalvi, L.V.A. and Vismara, M.V.G. (2012) Photo-Induced Dipole Relaxation Current in Natural Amethyst. *Materials Research*, **15**, 461-466. https://doi.org/10.1590/S1516-14392012005000052

[32] Chen, R. and Mckeever, S.W.S. (1997) Theory of Thermoluminescence and Related Phenomena. World Scientific, Singapore. https://doi.org/10.1142/2781

[33] Torizuka, K., Yamashita, M. and Yabiku, T. (1994) Thermal Effect in a Lamp-Pumped Continuous-Wave Alexandrite Laser. *Journal of Applied Physics*, **33**, 1899-1904. https://doi.org/10.1143/JJAP.33.1899

[34] Powell, R.C., Xi, L., Gang, X., Quarles, G.J. and Walling, J.C. (1985) Spectroscopy Properties of Alexandrite Crystals. *Physical Review B*, **32**, 2788-2797. https://doi.org/10.1103/PhysRevB.32.2788

[35] Suchocki, A.B., Gilliland, G.D., Powell, R.C., Bowen, J.M. and Walling, J.C. (1987) Spectroscopy Properties of Alexandrite Crystals II. *Journal of Luminescence*, **37**, 29-37. https://doi.org/10.1016/0022-2313(87)90179-7

[36] Scalvi, R.M.F. (2000) Electric Dipolar Relaxation in Natural and Synthetic Alexandrite. PhD Thesis, University of São Paulo, São Carlos.

Encontro de Física 2016

3 a 7 de setembro de 2016
Natal, Rio Grande do Norte

XIII EBFP XXXIX ENFMC XXXVII ENFPC XVI EPEF XXXIX RTFNB

CERTIFICADO

O Comitê Organizador certifica que o trabalho *Optical Absorption, Photoluminescence and Thermally Stimulated Depolarization Current studies on Cr+3 distribution in Al1 and Al2 sites of alexandrite (BeAl2O4:Cr3+).* de autoria de *NEILO MARCOS TRINDADE, ANA REGINA BLAK, ELISABETH MATEUS YOSHIMURA, LUIS VICENTE DE ANDRADE SCALVI, ROSA MARIA FERNANDES SCALVI* foi apresentado na sessão *INSULATORS AND DIELECTRICS*, no Encontro de Física 2016, realizado em Natal, RN, de 03 a 07 de Setembro de 2016, promovido pela Sociedade Brasileira de Física.

Natal, 7 de setembro de 2016.

168-21-2

SOCIEDADE BRASILEIRA DE FÍSICA

Ricardo Magnus Osório Galvão
Coordenador Geral

BMIC

São Pedro-SP, Brazil- 25-30/09/2016

XVIII BMIC Brazilian Meeting on Inorganic Chemistry • TR-2016 7th Brazilian Meeting on Rare Earths

Certificate of Presentation

We certified that the work entitled ***Photoluminescence and Thermoluminescence of Alexandrite ($BeAl_2O_4$:Cr^{3+})****, by TRNDADE, N. M.; SCALVI, L. V. A.; SCALVI, R. M. F.; BLAK, A. R.; YOSHIMURA, E. M. was presented as a Poster at the XVIII BMIC - Brazilian Meeting on Inorganic Chemistry and 7th Brazilian Meeting on Rare Earths, held at Hotel Colina Verde, São Pedro – SP, Brazil, from September, 25-30th, 2016.*

Sidney J.L. Ribeiro
(Chair)

CBECiMat

CBECiMat
Congresso Brasileiro de Engenharia e Ciência dos Materiais
06 a 10 de Novembro de 2016
Natal - RN - Brasil

CERTIFICADO

119-036

Certificamos que **Trindade, N.M.; Blak, A.R.; Yoshimura, E.M.; Scalvi, L.V.A.; Scalvi, R.M.F.;**
são autores do trabalho **TERMOLUMINESCÊNCIA (TL) E LUMINESCÊNCIA OPTICAMENTE ESTIMULADA (OSL) DE ALEXANDRITA (BEAL2O4:CR3+)**, apresentado por **Neilo Marcos Trindade,** no Congresso Brasileiro de Engenharia e Ciência dos Materiais de 06 a 10 de Novembro de 2016 -Natal – RN – Brasil.

CAPES

FAPESP
Fundação de Amparo à Pesquisa do Estado de São Paulo

Clodomiro Alves Jr.
Presidente do 22º CBECIMAT

VISUALIZAÇÃO DE DESPACHO

Processo	2016/22984-0
Linha de Fomento	Programas Regulares / Auxílios a Pesquisa / Participação em Reunião Científica ou Tecnológica / Reunião no Exterior - Fluxo Contínuo
Situação	Em Execução
Vigência	20/03/2017 a 22/03/2017
Beneficiário	Neilo Marcos Trindade
Responsável	Neilo Marcos Trindade
Vínculo Institucional do Processo	Instituto de Física/IF/USP

Folha de Despacho para Reconsideração 002 - Reunião no Exterior

Resultado

Concedido

Datas do Despacho

Emitido em : 03/02/2017

Orçamento Consolidado

Benefícios	Solicitado		Despacho	
	Valor (R$)	Valor (US$)	Valor (R$)	Valor (US$)
Custeio				
Despesas de Transporte	2.217,89	0,00	2.217,89	0,00
Diárias	0,00	750,00	0,00	750,00
Seguro Saúde	46,50	0,00	46,50	0,00
Taxas de Inscrição	0,00	592,28	0,00	613,83
Total	2.264,39	1.342,28	2.264,39	1.363,83
Total Geral	2.264,39	1.342,28	2.264,39	1.363,83

Dados de Execução

Data Início	20/03/2017
Duração	3 dia(s)
Data Término	22/03/2017
Área de alocação de recursos	Física
Relatório Científico (Quantidade)	1
Relatório Científico (Datas)	30/04/2017
Prestação de Contas (Quantidade)	1
Prestação de Contas (Datas)	30/04/2017

Observações / Transcrições / Frases

Observações ao Responsável

Comunicamos a V. Sa. que sua solicitação, constante do processo acima referido, foi analisada pela FAPESP, tendo sido aprovada.

Cabe-nos informar que alguns dos itens orçamentários podem não ter sido aprovados, ou aprovados com valores inferiores, por isso deve-se aguardar o Termo de Outorga com os valores finais concedidos.

Por favor, para qualquer consulta ou comunicação sobre esta correspondência, use exclusivamente os serviços do "Converse com a FAPESP" em www.fapesp.br/converse.

Atenciosamente,

Carlos Henrique de Brito Cruz
Diretor Científico da FAPESP

OBSERVAÇÕES:

Obs.1: "Cabe ao Outorgado obter da Instituição a que se vincula a autorização competente para o afastamento."

Frases para o Responsável

Não há frases associadas.

Transcrição de Parecer para o Responsável

Não há transcrição associada.

Frases para Termo de Outorga

Não há frases associadas.

Orçamento Detalhado - Quadros Resumos

Despesas de Transporte - Nacional

Item	Descrição	Solicitado			Despacho		
		Qtd	Valor Unitário (R$)	Valor Total(R$)	Qtd	Valor Unitário (R$)	Valor Total(R$)
1	Deslocamento aereo ida e volta: São Paulo - Cidade do Cabo.	1	2.217,89	2.217,89	1	2.217,89	2.217,89
Total				2.217,89			2.217,89

Despesas de Transporte - Importado

Nenhum benefício encontrado.

Diárias - Nacional

Nenhum benefício encontrado.

Diárias - Importado

Item	Descrição	Solicitado				Despacho			
		MO* / Tx. Conv. (US$)	Qtd	Valor Unitário	Valor Total(US$)	MO* / Tx. Conv. (US$)	Qtd	Valor Unitário	Valor Total(US$)
1	O congresso será realizado de 20 a 22/03.	US$/1,0000000	3	250,00	750,00	US$/1,0000000	3	250,00	750,00
Total					750,00				750,00

* MO = Moeda de Origem

Taxas de Inscrição - Nacional

Nenhum benefício encontrado.

Taxas de Inscrição - Importado

Item	Descrição	Solicitado				Despacho			
		MO* / Tx. Conv. (US$)	Qtd	Valor Unitário	Valor Total(US$)	MO* / Tx. Conv. (US$)	Qtd	Valor Unitário	Valor Total(US$)
1	REGISTRATION FEES Authors: £570	EUR/1,0391000	1	570,00	592,28	EUR/1,0769000	1	570,00	613,83

Total	592,28	613,83

* MO = Moeda de Origem

Seguro Saúde

Moeda R$

Justificativa

	Solicitado	Despacho
Valor Total	46,50	46,50

Orçamento Detalhado - Itens de despesa

Despesas de Transporte - Nacional

Origem	Brasil
Quantidade	1
Descrição	Deslocamento aereo ida e volta: São Paulo - Cidade do Cabo.
Valor Unitário	2.217,89
Valor Total	2.217,89
Justificativa	Anexo pre_plano_aereo em Outros Documentos.

Diárias - Importado

Quantidade	3
Descrição	O congresso será realizado de 20 a 22/03.
Local	Exterior
Moeda	US$
Valor Unitário	250,00
Valor Total	750,00
Justificativa	O congresso será realizado de 20 a 22/03, porém em virtude do tempo de deslocamento (passagens promocioniais) é necessário viajar com 2 dias de antecedência.

Taxas de Inscrição - Importado

Origem	Exterior
Quantidade	1
Descrição	REGISTRATION FEES Authors: £570
Moeda de Origem	EUR
Valor Unitário	570,00
Taxa de Câmbio (US$)	1,0769000
Valor Total	613,83
Justificativa	

Seguro Saúde

Moeda	R$
Valor Total	46,50
Justificativa	